





Integrating two-dimensional water temperature simulations into a fish habitat model to improve hydro- and thermopeaking impact assessment

Manuel Antonetti¹  | Luca Hoppler¹ | Diego Tonolla¹  | Davide Vanzo^{2,3}  |
Martin Schmid²  | Michael Doering¹

¹Institute of Natural Resource Sciences, Zurich University of Applied Sciences (ZHAW), Wädenswil, Switzerland

²Department of Surface Waters – Research and Management, Eawag, Kastanienbaum, Switzerland

³Swiss Federal Institute of Technology, Laboratory of Hydraulics, Hydrology and Glaciology, Zurich, Switzerland

Correspondence

Manuel Antonetti, Institute of Natural Resource Sciences, Zurich University of Applied Sciences (ZHAW), Grüental, 8820 Wädenswil, Switzerland.

Email: manuel.antonetti@zhaw.ch

Funding information

Swiss Federal Institute of Aquatic Science and Technology (Eawag)

Abstract

Storage hydropower plants, which are an important component of energy production in Switzerland, can lead to hydro- and thermopeaking, affecting river habitats and organisms. In this study, we developed an approach for integrating water temperature simulations into a habitat model to assess the impact of both hydro- and thermopeaking on the availability of suitable fish habitats. We focused on the habitat requirements of juvenile brown trout (*Salmo trutta*) in a semi-natural braided floodplain along the Moesa River (Southern Switzerland) in early summer. First, we defined different scenarios (with and without hydropeaking) based on the local hydrological and meteorological conditions. Second, we used a two-dimensional depth-averaged hydro- and thermodynamic model to simulate the spatial distributions of water depth, flow velocity, and water temperature. Third, we applied generalized preference curves for juvenile brown trout to identify hydraulically suitable habitats, and developed a new index to assess the availability of thermally suitable habitats. Finally, we quantified the extent to which hydraulically and thermally suitable habitats overlap in space and time. During both base and peak flow phases, most of the hydraulically and thermally suitable habitats are located in the side channels. High flow conditions combined with strong cold-thermopeaking lead to a higher thermal heterogeneity. However, disconnected habitats originate in the dewatering zone, increasing the risk of stranding as well as thermal stress. By helping to better understand the effects of thermopeaking on the availability of fish habitats, our approach could contribute to the design and evaluation of ecological restoration in hydropeaking rivers.

KEYWORDS

brown trout, habitat suitability curves, hydropeaking, *Salmo trutta*, Switzerland, thermodynamic simulation, thermopeaking, thermoregulation

This is an open access article under the terms of the [Creative Commons Attribution-NonCommercial-NoDerivs](https://creativecommons.org/licenses/by-nc-nd/4.0/) License, which permits use and distribution in any medium, provided the original work is properly cited, the use is non-commercial and no modifications or adaptations are made.

© 2022 The Authors. *River Research and Applications* published by John Wiley & Sons Ltd.

1 | INTRODUCTION

Hydropower is an important renewable energy source contributing ca. 16% to the global and ca. 60% to Swiss electricity production (International Energy Agency, 2019; Swiss Federal Office of Energy, 2020). Hydropower facilities thus play a crucial socio-economic role, but they also impact rivers by altering their hydrological and sediment regimes (Poff et al., 1997; Wohl et al., 2015). In particular, intermittent electricity production of storage hydropower plants results in daily and sub-daily flow fluctuations (“hydropeaking”). In contrast to natural flow variability due to snowmelt or rainfall, hydropeaking events are more frequent (Greimel et al., 2016). They have multiple and complex effects on river ecosystems, including impacts on riparian vegetation (reviewed by Bejarano, Jansson, & Nilsson, 2018), drift and stranding of aquatic organisms (e.g., macroinvertebrates and fish), and reduced reproductive success in fish (Bruder et al., 2016; Moreira et al., 2019; Schmutz et al., 2015; Young, Cech, & Thompson, 2011).

The temperature of turbinized water from storage hydropower plants usually differs from the downstream river, causing sharp alterations in water temperature, that is, thermopeaking (Toffolon, Siviglia, & Zolezzi, 2010; Zolezzi, Siviglia, Toffolon, & Maiolini, 2011). River water temperature is a key driver in aquatic ecosystems (Caissie, 2006). Related to storage hydropower plants, previous studies on thermal alterations examined the effects of long-term (seasonal) water temperature shifts. For example, rivers tend to be warmed up in winter and cooled down in summer by the water turbinized from reservoirs (Feng, Zolezzi, & Pusch, 2018; Heggenes, Alfredsen, Bustos, Huusko, & Stickler, 2018; Meier, Bonjour, Wuest, & Reichert, 2003; Olden & Naiman, 2010), with potential ecological consequences such as shifts in fish hatching periods (Angilletta Jr et al., 2008; Zhong & Power, 1996). Short-term (sub-daily) thermal variations were found to influence the distribution, behaviour, and survival of fish and other aquatic organisms (Bruno, Siviglia, Carolli, & Maiolini, 2013; Carolli, Bruno, Siviglia, & Maiolini, 2012; Halleraker et al., 2003; Saltveit, Halleraker, Arnekleiv, & Harby, 2001). In particular, the water temperature can influence fish performance, food intake, metabolism, growth, and reproduction (see for a review Jonsson & Jonsson, 2009). Several studies have documented the negative effects of cold water coming from reservoirs, such as the local disappearance of warm water fish (Quinn & Kwak, 2003), lower larval development (Clarkson & Childs, 2000), or reduced growth rates of juvenile fish (Saltveit, 1990), as well as the influence of thermopeaking on habitat selection, migration, spawning behaviour, larval development, or behavioural drift of fish (Moreira et al., 2019; Zolezzi et al., 2011).

To avoid thermal stress if temperatures are too high or too low, salmonids move to thermal refugia (Berman & Quinn, 1991; Breau, Cunjak, & Bremset, 2007; Petty, Hansbarger, Huntsman, & Mazik, 2012; Wilbur, O'Sullivan, MacQuarrie, Linnansaari, & Curry, 2020). However, they actively exploit the spatiotemporal heterogeneity of water temperature also outside the critical temperature range for regulating their internal temperature (Armstrong et al., 2013; Baldock, Armstrong, Schindler, & Carter, 2016; Brewitt,

Danner, & Moore, 2017). Elliott (1981) argued that this thermoregulatory behaviour (thermoregulation) is one of the main factors in fish movement, whereas Jonsson and Jonsson (2011) were critical of whether there is, in nature, a direct relationship between temperature for maximum growth efficiency and habitat selection in salmonids. Based on laboratory experiments, Elliott and Allonby (2013) showed that brown trout actively select temperatures for maximum growth, when the opportunity is given.

As the most widespread fish habitat model type, habitat suitability models have been increasingly used to assess the effects of hydropeaking on the availability of suitable fish habitats (García, Jorde, Habit, Caamaño, & Parra, 2011; Muñoz-Mas, Martínez-Capel, Schneider, & Mouton, 2012; Pisaturo et al., 2017; Weber, Schneider, Junker, Kopecki, & Alexander, 2015). Such models quantify the extension of suitable microhabitats in a river reach by combining the results of a hydrodynamic model with the habitat requirements of a target species. The most common variables used for fish habitat suitability models are water depth and flow velocity, and to a lesser extent, substrate (Eberstaller et al., 2012; Hauer, Unfer, Holzappel, Haimann, & Habersack, 2014; Jonsson & Jonsson, 2009; Person, Bieri, Peter, & Schleiss, 2014). Despite the lively interest in river water temperature research (Ouellet et al., 2020), few studies simulate the combined effects of hydraulic conditions and water temperature on the availability of suitable habitats in complex floodplains under hydropeaking conditions. Grand, Railsback, Hayse, and LaGory (2006) investigated the influence of water temperature and habitat geometry on the availability of nursery habitats for larval and juvenile Colorado pikeminnow (*Ptychocheilus lucius*) in the Green River, Utah. Furthermore, Casas-Mulet, Saltveit, and Alfredsen (2016) proposed a modelling approach to assess the impact of different mitigation strategies on the hydrological and thermal effects of hydropeaking on the early life stages of salmonids in the Lundesokna River (Norway), where flow and thermal conditions were simulated in a one-dimensional framework. However, these habitat modelling frameworks are hardly applicable for a hydro-thermopeaking impact assessment on study sites with complex morphologies, as the spatial heterogeneity of hydrodynamic and thermal conditions suggests a more refined, two-dimensional (2D) modelling approach. Ouellet, Secretan, St-Hilaire, and Morin (2014) employed a 2D hydro-thermal model to simulate St. Lawrence River dynamics on a daily scale. Similarly, Yao, Chen, Zhong, Zhang, and Fan (2017) assessed the impact of restoration strategies on the Mian River (China) by modelling hydrodynamics, sediment transport, and heat transfer in a 2D manner. However, they focussed on the long-term effects.

In this study, we developed an interdisciplinary approach for integrating 2D depth-averaged water flow and temperature simulations into a fish habitat model, with the aim of assessing the combined effect of both hydro- and thermopeaking on the availability of suitable fish habitats. Hydro-thermodynamic simulations were conducted with the freeware tool BASEMENT (Vanzo et al., 2021), equipped with a dedicated module for water temperature simulations. For the habitat modelling, we focused on the habitat requirements of juvenile brown trout (*Salmo trutta*) in a semi-natural braided floodplain along the

Moesa River (Southern Switzerland) during early summer conditions. In this period, the mean water temperature is still below the values that are optimal for metabolism and thus provide a growth advantage for juvenile brown trout (Elliott & Allonby, 2013). We therefore assumed areas with higher relative temperatures (warm water patches) as being more suitable habitats for thermoregulation of juvenile brown trout, referred to hereafter as thermal suitable habitats. We addressed the following research questions: (a) How does the spatiotemporal availability of hydraulically and thermally suitable habitats for juvenile brown trout change with different hydrometeorological scenarios? (b) How does hydropeaking modify the spatial distribution of hydraulically suitable habitats for juvenile brown trout? (c) How does thermopeaking impact the thermal heterogeneity as well as the suitable habitats for thermoregulation?

2 | METHODS

2.1 | Study area and data collection

The Pomareda floodplain (46°20'00"N; 9°12'30"E) is located at 450 m a.s.l. along the Moesa River in the Canton of Grisons (Southern Switzerland, Figure 1). The Moesa is a fifth-order Alpine River that originates above the San Bernardino Pass at around 2,250 m a.s.l. and flows in the southern direction through the Mesolcina valley, ultimately draining into the Ticino River after ca. 43 km at 230 m a.s.l. While the upper section of the river upstream of the Isola reservoir (1,600 m a.s.l.) is minimally impacted or near natural, the middle and lower sections are morphologically heavily impacted. The Pomareda floodplain is

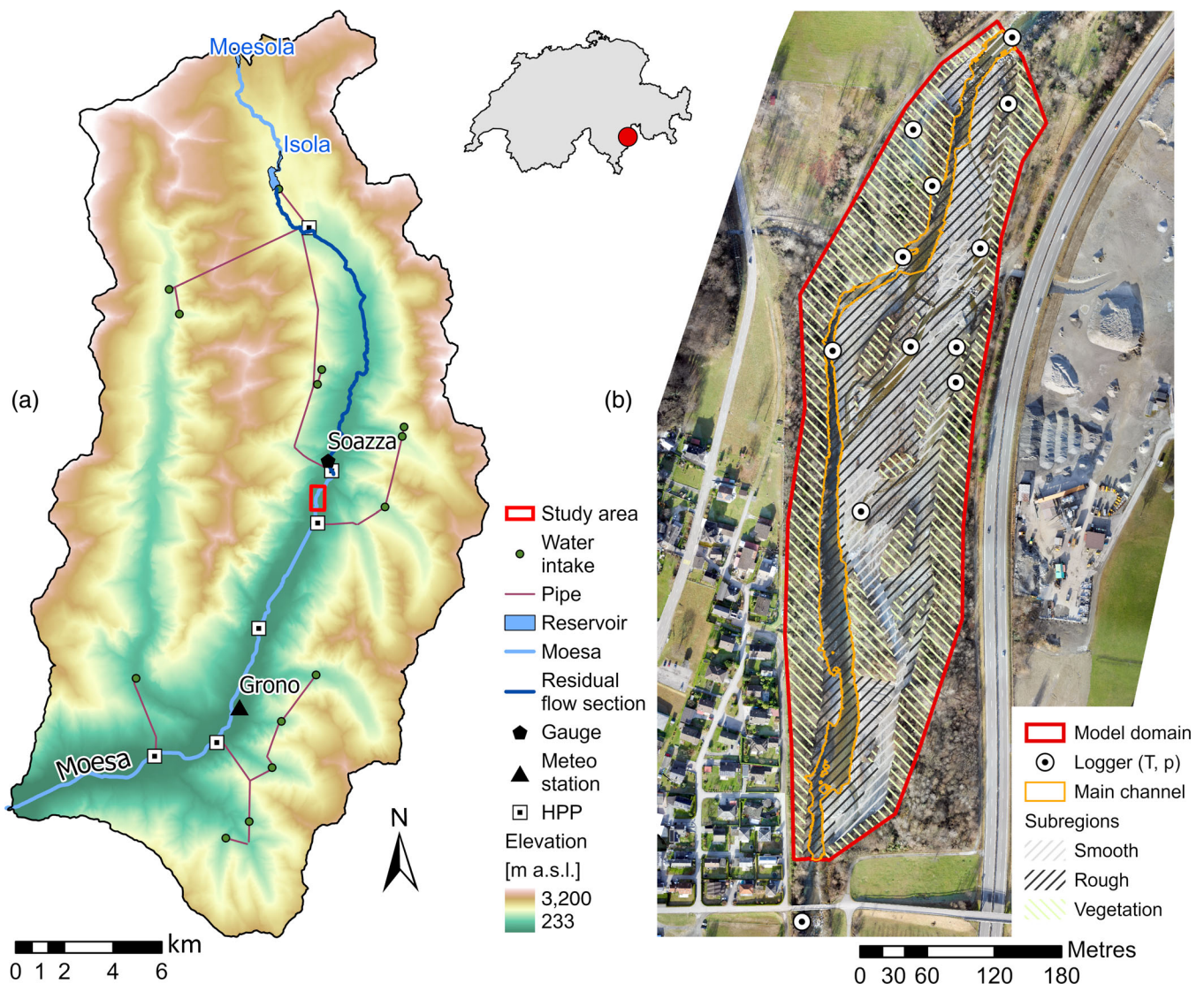


FIGURE 1 (a) Map of the Moesa catchment (Southern Switzerland), as well as the location of hydropower plants (HPP), reservoirs, water intakes, pipes, and residual flow section. The study area is outlined in red. Background map: DHM25 SwissTopo. (b) Overview of the Pomareda floodplain; location of the data loggers (water level and temperature), as well as computational domain and roughness subregions defined for the hydrodynamic modelling. Flow direction from north to south. Background map: Orthofoto of December 2018 [Color figure can be viewed at wileyonlinelibrary.com]

approximately 800 m long, with an averaged longitudinal slope of 0.012 (m/m) and floodplain width ranging between 100 and 200 m. The substrate is dominated by gravel (median diameter of 7 cm) with localized patches of sand. The reach is subject to hydropeaking due to the hydropower plant of Soazza, operating two turbines with a maximum production capacity of 7 m³/s each (Paszti, 2019). The turbined water is mainly diverted from the Isola reservoir (volume: 6.5 million m³; max. depth: 39 m), with minor contributions from the Calancasca River and other small tributaries (Figure 1). The Isola reservoir is exploited by Officine Idroelettriche di Mesolcina solely for hydropower electricity generation. According to Huet (1949), the river is located in the transition area between the lower trout (*S. trutta*) and the upper grayling (*Thymallus thymallus*) regions, but also bullhead (*Cottus gobio*) are present in the area (personal communication from Flavio Nollo, resp. Mesolcina valley at the Ufficio Caccia e Pesca of the Canton of Grisons).

The topography of the study area was derived by a drone (UAV) survey in December 2018 at low flow conditions of 2.0 m³/s using an eBee Classic™ equipped with an RGB camera (S.O.D.A). A total of 14 ground control points were measured by an RTK-GPS (Trimble R10 GNSS system; accuracy < 2 cm) for orthorectification. Drone images were processed with Pix4D mapper (Pix4D, 2020) to extract a digital elevation model (DEM). The bathymetric data of the river floodplain was integrated into the DEM based on further RTK-GPS measurements.

Water levels were available from a gauging station at Soazza Al Pont (SEBA Hydrometrie GmbH & Co., 2021) located in the residual flow section, approximately 4 km upstream of the study site. These were converted into discharge data based on a rating curve derived from flow measurements performed at three different discharges (Paszti, 2019). With the derived rating curve, the discharge averages approximated 4 m³/s during summer time and 1.5 m³/s during winter (van Rooijen, 2022). Turbined water flow data from the hydropower plant was available with a resolution of 3 min for the investigated period. Water level and temperature were continuously measured by 12 data loggers (HOBO U20L-04, water level and temperature accuracy of 0.4 cm and 0.44°C, respectively) installed in the main and side channels of the floodplain, whereas for air temperature, global radiation, wind speed, and relative humidity, data from the automatic meteorological station at Grono (323 m a.s.l.; MeteoSwiss, 2020) was used (Figure 1). Moreover, thermal infrared (TIR) UAV surveys were performed in February 2019 using an eBee Classic™ equipped with a TIR camera (thermoMAP).

2.2 | Hydro- and thermodynamic modelling

For the hydrodynamic modelling we used the modular freeware BASEMENT v3 (V3.0.1; Vanzo et al., 2021), which solves the 2D shallow water equations with a finite volume method on unstructured computational meshes. A newly developed numerical module was implemented for the simulation of thermodynamic processes. The

module solves the transport and mixing of water temperature with a scalar advection–diffusion equation solver based on a relaxation approach described in Vanzo, Siviglia, and Toro (2016). The module can additionally evaluate atmospheric forcing terms to resolve the heat exchange at the water–air interface. A summary of the governing equations and closure relationships is given in the Supporting Information.

The model does not account for the fluid mass loss due to evaporation or infiltration, as it is often negligible in practical applications. As consequence, fictitious high temperatures might occur in almost-dry cells having vanishing flow velocity. To overcome such numerical inaccuracies, the analysis of the simulation results is restricted to computational cells with water depths greater than 0.05 m. For these cells, the spatial median of the simulated water temperatures, as well as the coefficient of quartile variation (CQV; Bonett, 2006) as a measure of thermal heterogeneity, were calculated at 15-min intervals. Hyporheic and/or groundwater exchanges, which might increase or decrease thermal heterogeneity (Malard, Mangin, Uehlinger, & Ward, 2001; Olsen & Young, 2009; Uehlinger, Malard, & Ward, 2003; Wawrzyniak, Piégay, Allemand, Vaudor, & Grandjean, 2013), were not considered in the model. In support of this modelling assumption, the TIR-UAV surveys in conjunction with local water temperatures from the data loggers did not reveal relevant upwelling phenomena in the study area (Figure A1).

The Pomereda floodplain was discretized with a total of 175,520 computational cells with a mean cell size of 0.62 m². In terms of hydrodynamic boundary conditions (BCs), a total discharge volume was provided at the inflow as a hydrograph, whereas for the outflow BC a uniform flow was imposed. The computational domain was divided into three roughness subregions (“smooth,” “rough,” and “vegetation”) and, for each one, a Strickler friction coefficient was assigned (55, 30, and 5 m^{1/3}/s respectively, Figure 1). The roughness coefficients were calibrated over three different discharge stages against five different water level measurements in the floodplain. Two additional water level measurements were used for validation. The mean average error was <5 cm in both calibration and validation. Further details can be found in Paszti (2019) and van Rooijen (2022). The Courant–Friedrichs–Lewy number was set to 0.95. Concerning the BCs for the thermodynamic simulations, the inflowing water temperature was provided as temporal series, whereas zero gradients (i.e., Neumann type) BCs were set at the outflow. For the calculation of the atmospheric forcing terms, temporal series of air temperature, global radiation, and wind speed were provided (see Section 2.4).

2.3 | Fish habitat modelling

To model the extent of hydraulically suitable habitats, empirically-derived habitat suitability curves (HSC) are generally used to quantify habitat preferences for different abiotic parameters and different life stages on a scale between 0 (complete avoidance) and 1 (best suitability; Wakeley, 1988; Person et al., 2014; Macura, Štefunková,

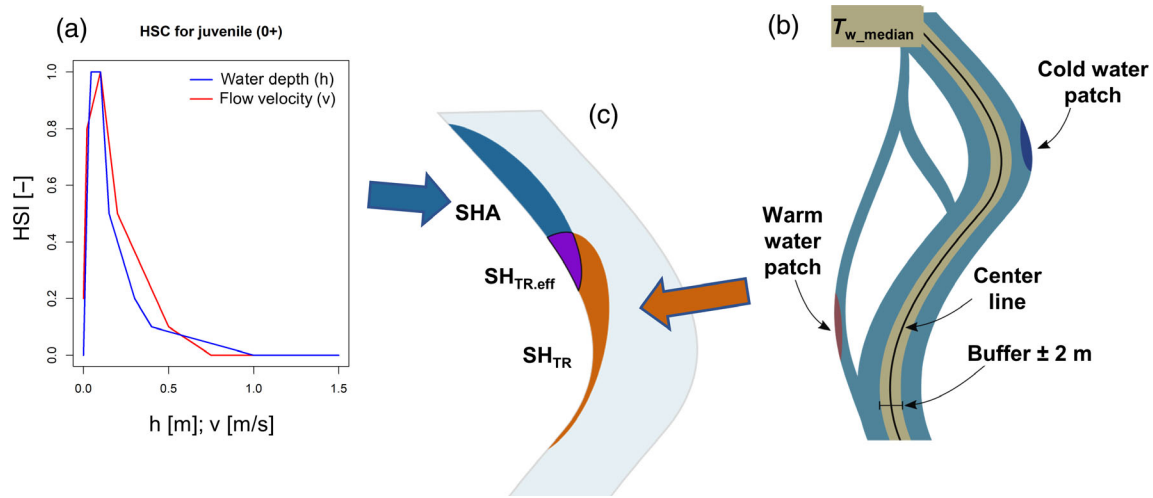


FIGURE 2 Schematic representation of the habitat modelling approach. (a) Generalized habitat suitability curves (HSC) after Hauer et al. (2014) indicate the habitat suitability index (HSI) corresponding to a given water depth (h) or flow velocity (v). These are used to identify hydraulically suitable habitats (SHA). (b) Warm water patches are identified according to Wawrzyniak et al. (2016) and are assumed to be suitable habitats for thermoregulation (SH_{TR} ; $T_{w,median}$ = median of water temperature). (c) The overlapping area between SHA and SH_{TR} represents the effective suitable habitats for thermoregulation ($SH_{TR,eff}$) [Color figure can be viewed at wileyonlinelibrary.com]

Majorošová, Halaj, & Škrinár, 2018). As no HSCs are available specifically for the study area, we used the generalized HSCs for the early development stages (0+) of brown trout after Hauer et al. (2014; Figure 2a). As parameters, we account for water depth and flow velocity only, given that sediment texture is quite homogeneous in the study area. To compare the availability of hydraulically suitable habitats at different discharges, the habitat suitability index (HSI), the suitable habitat area (SHA), and the suitable habitat ratio (SHR) were calculated based on the simulation results (Person et al., 2014; Table A2). The HSI (–) is calculated as the geometric mean of the suitability indices of water depth and flow velocity for each computational cell at a given discharge. The SHA (m^2) represents the total area of suitable habitat and is calculated by adding up the areas of all computational cells with an HSI > 0.5. The SHR (–) is the ratio between the SHA and the effective wetted area (WA [m^2] of computational cells with a water depth > 0.05 m) for a given discharge.

Changes in the spatial distribution of hydraulically suitable habitats during hydropeaking scenarios were assessed by quantifying the change in SHA over the course of the day for the permanently wetted zone (i.e., base flow zone) and the dewatering zone. Moreover, the spatial distribution of hydraulically suitable habitats was analysed by comparing their spatial extension during both base (Q_{base}) and peak flow (Q_{peak}). Those habitats remaining suitable during both Q_{base} and Q_{peak} were considered “stable,” whereas those suitable either during Q_{base} or Q_{peak} were considered “unstable” and “new,” respectively.

With regard to the suitable habitats for thermoregulation, the thermal anomalies in the floodplain were detected, in a first step, following Wawrzyniak et al. (2016; Figure 2b). The median temperature within a 2 m buffer around the centreline of the main channel was calculated and the thermal anomaly for each computational cell was

computed as the difference to this value. Cells with a thermal anomaly of at least $\pm 0.5^\circ C$ were classified as warm- or cold-water patches. In a second step, suitable habitats for thermoregulation (SH_{TR} [m^2]) were determined based on these thermal anomalies. We considered a computational cell to be suitable for thermoregulation if its thermal anomaly is positive (i.e., warm water patch) and its water temperature does not exceed a given preferential temperature threshold ($T_{w,pref}$) for juvenile brown trout. This temperature depends on several factors, such as time of day or food intake (Elliott & Allonby, 2013). For the present study, a constant value of $16^\circ C$ was assumed as $T_{w,pref}$. As we focussed on early summer conditions, when temperatures never fall below the lower optimum threshold ($4^\circ C$ according to Elliott, 1981), there was no need to set one for our analysis. SH_{TR} was calculated for the entire floodplain for each simulation time step and its temperature range (i.e., the interval between $T_{w,median} + 0.5^\circ C$ and $T_{w,pref}$) compared with the corresponding cumulative water temperature distribution. Moreover, the SHR for thermoregulation (SHR_{TR} [–]) was calculated as the ratio between SH_{TR} and the WA for a given discharge, this allowed for different hydrometeorological scenarios to be compared. To determine whether suitable habitats for thermoregulation overlap in space and time with those hydraulically suitable, the overlapping area of SH_{TR} and SHA was calculated for each scenario and time step. These areas are referred to as effective suitable habitats for thermoregulation ($SH_{TR,eff}$, Figure 2c).

2.4 | Simulation scenario design

In an initial step, steady-state discharge conditions between 2 and $20 m^3/s$ were simulated with a $1 m^3/s$ step to assess the extent of SHA over the whole discharge range that could occur in the Pomareda floodplain during hydropeaking (flood discharges were neglected). In a

TABLE 1 Overview of the parameter values used for the 15 scenarios simulated in this study (M1, M2, and M3 = sub-scenarios defined based on synthetic meteorological conditions; QR = sub-scenarios defined based on hydrological conditions on the residual flow section; HP = sub-scenarios defined based on the discharge of the water turbined from the hydropower plant; and TP = sub-scenarios defined based on the temperature of the water turbined from the hydropower plant)

Scenario	Base flow (Q_{base})			Peak flow (Q_{peak})		Meteorological conditions		
	Q (m^3/s)	T_{w_mean} ($^{\circ}C$)	T_{w_amp} ($^{\circ}C$)	Q_{amp} (m^3/s)	T_{w_TP} ($^{\circ}C$)	T_{a_mean} ($^{\circ}C$)	T_{a_amp} ($^{\circ}C$)	GR_{max} (W/m^2)
M1_QR2_HP0	2	9.5	1	—	—	20	4	600
M1_QR4_HP0	4	9.5	1	—	—	20	4	600
M1_QR6_HP0	6	9.5	1	—	—	20	4	600
M2_QR2_HP0	2	9.5	2	—	—	20	6	800
M2_QR4_HP0	4	9.5	2	—	—	20	6	800
M2_QR6_HP0	6	9.5	2	—	—	20	6	800
M3_QR2_HP0	2	9.5	3	—	—	20	8	1,000
M3_QR4_HP0	4	9.5	3	—	—	20	8	1,000
M3_QR6_HP0	6	9.5	3	—	—	20	8	1,000
M2_QR4_HP7_TP4	4	9.5	2	7	4	20	6	800
M2_QR4_HP7_TP6	4	9.5	2	7	6	20	6	800
M2_QR4_HP7_TP8	4	9.5	2	7	8	20	6	800
M2_QR4_HP14_TP4	4	9.5	2	14	4	20	6	800
M2_QR4_HP14_TP6	4	9.5	2	14	6	20	6	800
M2_QR4_HP14_TP8	4	9.5	2	14	8	20	6	800

Note: The parameter values were gradually adjusted starting from the scenario “M2_QR4_HP0” (bold).

Abbreviations: GR_{max} , daily maximum of global radiation; Q , discharge; Q_{amp} , amplitude of the hydropeaking event, defined as $Q_{peak} - Q_{base}$; T_{w_mean} , mean daily water temperature; T_{a_mean} , mean daily air temperature; T_{w_amp} , amplitude of daily water temperature; T_{a_amp} , amplitude of daily air temperature.

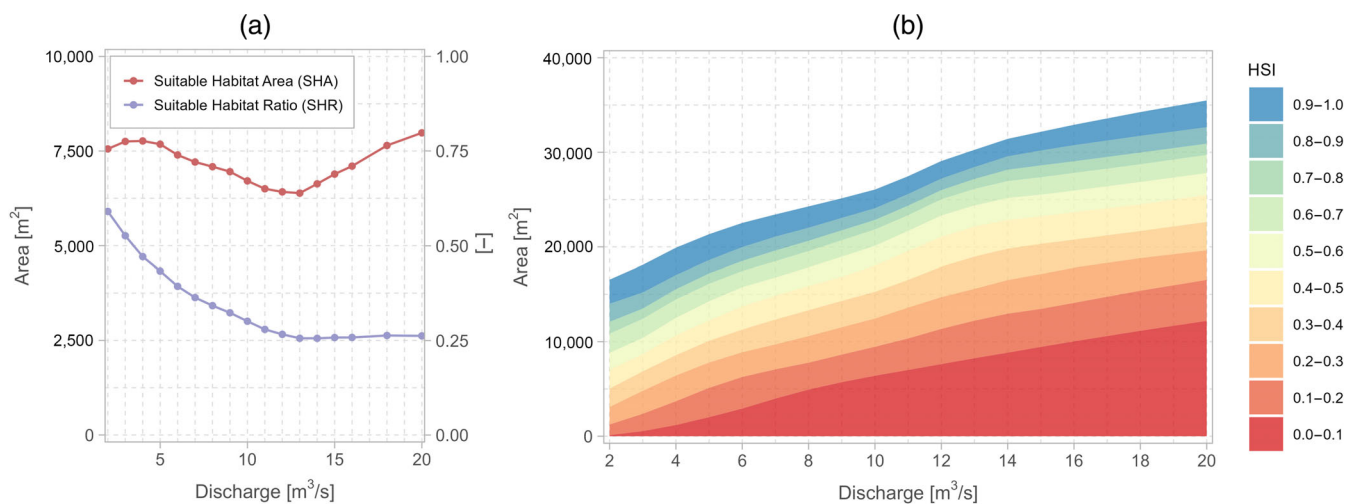


FIGURE 3 (a) Suitable habitat area (SHA, red line) and suitable habitat ratio (SHR, blue line) for juvenile brown trout as a function of discharge. (b) Wetted area as a function of discharge, subdivided into habitat suitability index (HSI) classes for juvenile brown trout [Color figure can be viewed at wileyonlinelibrary.com]

second step, synthetic hydrometeorological scenarios were simulated with different daily time series of water temperature, air temperature, and global radiation under three constant base flows (Table 1). To reproduce early summer hydraulic and thermal conditions as realistic as possible, we analysed the hydrological and meteorological observations in the study area between May and June and derived three base

flows ($Q_{base} = 2, 4, \text{ and } 6 \text{ m}^3/s$) and three meteorological scenarios, all which were then combined (Table 1). For the meteorological scenarios, the June 5, 2019 was selected as a representative day, as its summary statistics (min, max, and mean) were the closest to those of the whole time period considered. The corresponding measured data was used to derive synthetic daily time series (see Figure A2). For the

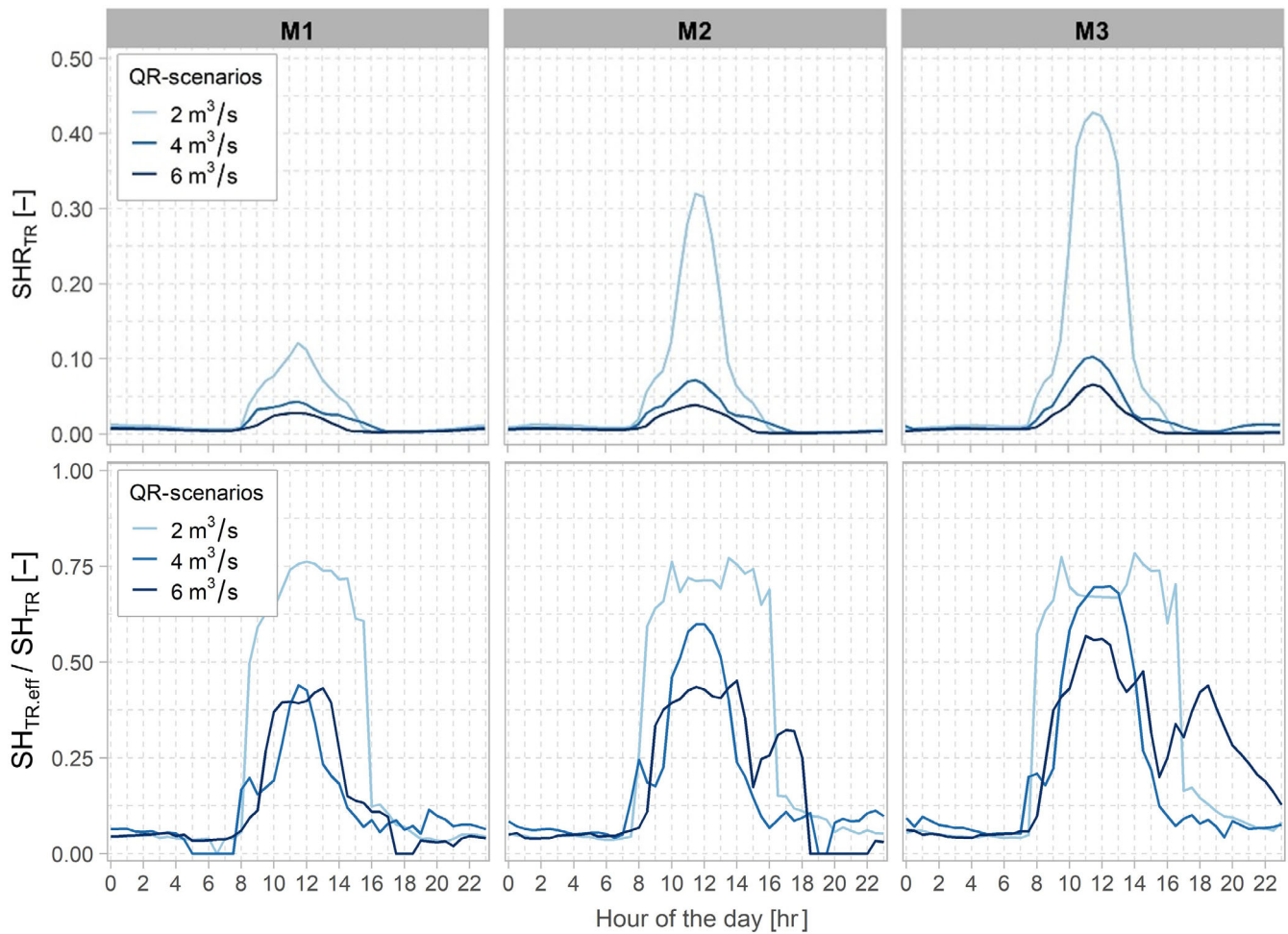


FIGURE 4 Suitable habitat ratio for thermoregulation (SHR_{TR} ; above) and the ratio of the effective suitable habitats for thermoregulation ($SH_{TR,eff}$) to the suitable habitats for thermoregulation (SH_{TR} ; below) over the course of the day for different hydrological (QR) and meteorological (M) scenarios (without hydropeaking) [Color figure can be viewed at wileyonlinelibrary.com]

global radiation, we fitted a Gaussian function to the measured data, whereas for the air and water temperature we used a sine function (Table A3). To reduce the computational effort, we restricted the simulations to three meteorological scenarios (M1, M2, and M3). Starting from the scenario that best reproduced the selected representative day (i.e., M2), two further scenarios were defined to reproduce a typical colder and cloudier day (M1), as well as a warmer and sunnier one (M3; Table A1 and Figure A2). Compared to M2, a smaller amplitude of daily air temperature ($T_{a,amp}$), a smaller one of water temperature ($T_{w,amp}$), and a lower daily maximum of global radiation (GR_{max}) were assigned to M1. In contrast, higher values of $T_{a,amp}$, $T_{w,amp}$, and GR_{max} than M2 were defined for M3. For all scenarios, we kept wind speed constant at 2 m/s, as a sensitivity analysis it did not show relevant effects on the model output (see Figure A3).

To investigate the impact of hydro- and thermo-peaking, we defined, in a third step, a total of six scenarios based on the available hydropower turbined water flow data (Table 1). These consist of two hydropeaking hydrographs with different amplitudes ($Q_{amp} = 7$ and 14 m³/s according to the production capacity of the turbines). Based

on an analysis of the turbined water flow data, the number of peaks (2), peak duration (3 hr), and time of day (morning and evening), as well as the up- and down-ramping rates (± 1.4 m³/s per minute) were considered representative for the hydropower plant at Soazza and kept constant during the simulations. The temperature of the water turbined from the hydropower plant could only be estimated indirectly by comparing the temperatures of the data loggers in the floodplain during the peak phases. These show that, between February and May, the temperature of the water turbined from the hydropower plant was always lower compared to the water in the floodplain. As the daily mean water temperature in the floodplain was set at 9.5°C, we defined three scenarios with constant water temperatures of 4, 6, and 8°C for the water turbined from the hydropower plant (Table 1).

For the input water temperature, we assumed the turbined and the residual flow water to be well mixed at the beginning of the computational domain (about 700 m downstream of the turbine outlet, Figure 1). The input temperature of the different scenarios was therefore calculated as a mixing ratio of discharge and

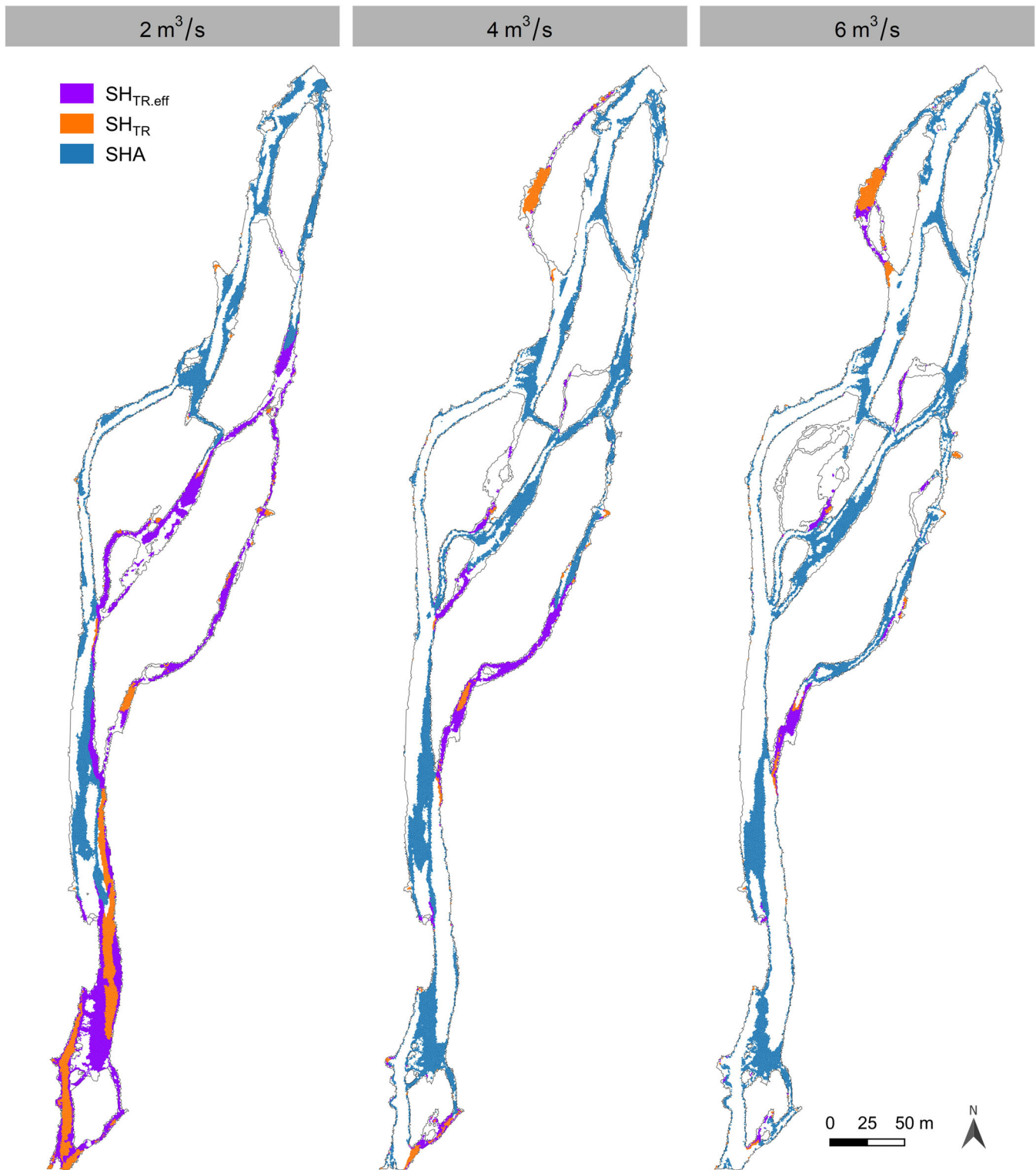


FIGURE 5 Spatial distribution of the hydraulically suitable habitats (SH), those suitable for thermoregulation (SH_{TR}), and the overlap between them ($SH_{TR,eff}$) at 11:30 a.m. for juvenile brown trout in the M3 scenario for three different base flows (2, 4, and $6 \text{ m}^3/\text{s}$). Flow direction from north to south. The location of the main channel is depicted in Figure 1 [Color figure can be viewed at [wileyonlinelibrary.com](https://onlinelibrary.wiley.com)]

temperature (see Table A3). All the scenarios with thermopeaking were simulated with a base flow of $4 \text{ m}^3/\text{s}$. The water temperature in the floodplain at the simulation start was set at 9.5°C , and a

warm-up period of 86,400 s (1 day) was included in the simulations to allow the computational domain to reach an equilibrium state with the external forcing.

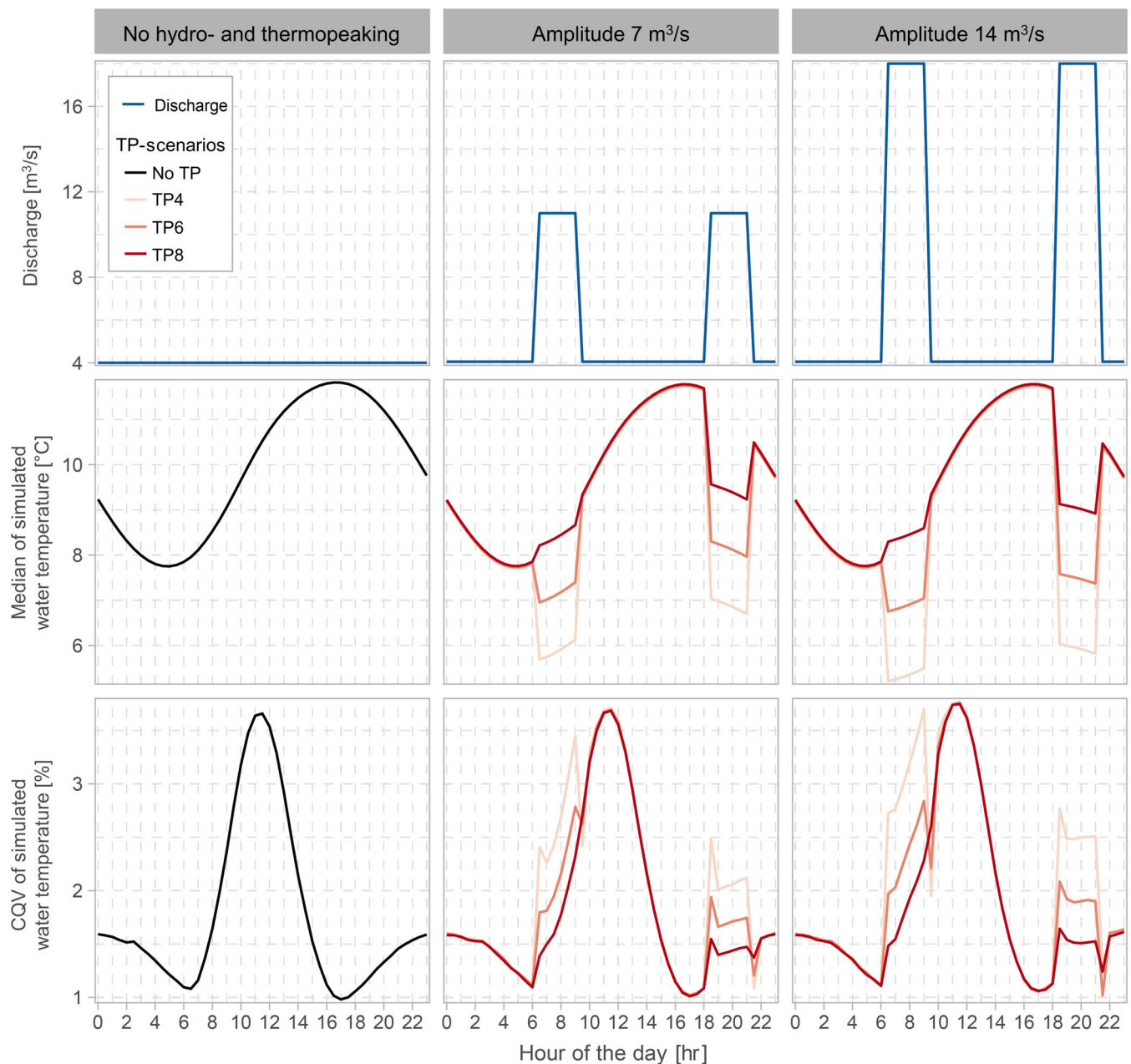


FIGURE 6 Total discharge volume entering the computational domain (top), median (middle), and coefficient of quartile variation (CQV; bottom) of simulated water temperatures over the course of the day without (left) and with (right and centre) hydropeaking (base flow $4 \text{ m}^3/\text{s}$). The scenarios differed in amplitude (7 and $14 \text{ m}^3/\text{s}$) and in temperature of the turbined water (TP4 = 4°C , TP6 = 6°C , and TP8 = 8°C), see Table 1 [Color figure can be viewed at wileyonlinelibrary.com]

3 | RESULTS

3.1 | Spatiotemporal availability of suitable habitats under different hydrometeorological scenarios

The SHA in the Pomareda floodplain remained relatively constant for the modelled discharges (Figure 3a). The highest values were reached at discharges of 2–5 and 19–20 m^3/s . As the WA increased with increasing discharge (Figure 3b), the SHR decreased from ca. 60% at a

discharge of 2 m^3/s to ca. 25% at 20 m^3/s . Between 13 and 20 m^3/s , the SHR remained relatively constant, as the SA increased proportionally to WA. Areas with very high suitability (HSI > 0.9) were present to a similar extent at all discharges. In contrast, areas that are very likely avoided by juvenile brown trout (HSI < 0.1) increased markedly with increasing discharge (Figure 3b).

SHR_{TR} were mainly present during the daylight hours in all scenarios (Figure 4, top), with a maximum around noon. The highest values were found at 2 m^3/s in scenario M3 with a maximum of ca. 40% of the WA, corresponding to about 5,500 m^2 . With lower

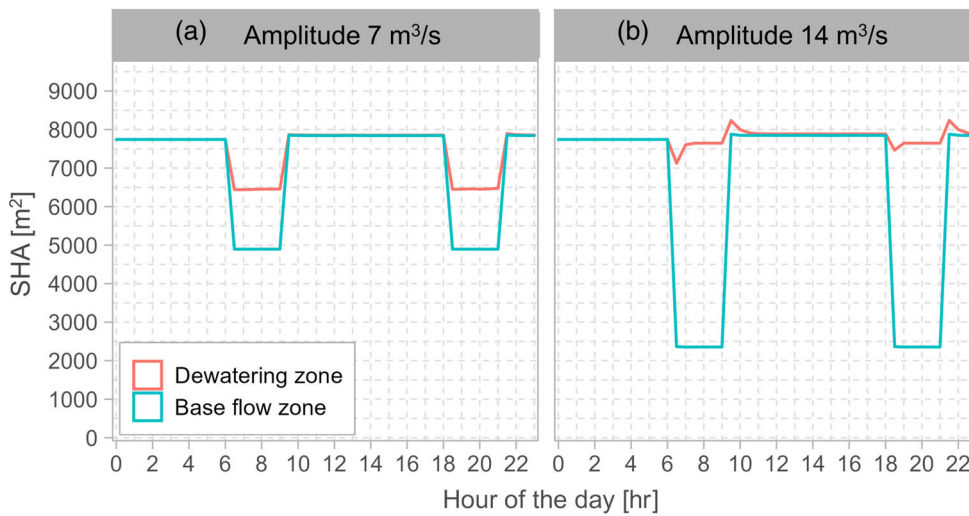


FIGURE 7 Total area of hydraulically suitable habitats (SHA, top) for juvenile brown trout over the course of the day and spatial distributions of unstable, new, and stable SHA (bottom) for two different amplitudes: (a) One turbine working and (b) both turbines working; base flow $4 \text{ m}^3/\text{s}$ [Color figure can be viewed at wileyonlinelibrary.com]



temperature amplitudes and lower global radiation maxima, as well as with higher discharges, SHR_{TR} decreased markedly. The smallest SHR_{TR} was found in scenario M1 at $6 \text{ m}^3/\text{s}$, with a maximum of 3% of WA (500 m^2). Effective suitable habitats for thermoregulation were present in all scenarios (Figure 4, bottom). At $2 \text{ m}^3/\text{s}$ during the day, nearly 75% of SH_{TR} was hydraulically suitable, too. With increasing discharge, this ratio decreased, whereas the meteorological conditions (i.e., air temperature and global radiation) had a less marked influence.

The spatial distribution of SHA was similar among the three base flows (Figure 5). With increasing discharge, however, the availability of suitable habitats in the main channels decreased. While at $2 \text{ m}^3/\text{s}$ the extent of suitable habitats in the main channel and in the side channels was similar, at 4 and $6 \text{ m}^3/\text{s}$ the $\text{SH}_{\text{TR,eff}}$ was more widespread in the side channels than in the main one. The largest $\text{SH}_{\text{TR,eff}}$ was expected in the side channels with $2 \text{ m}^3/\text{s}$ and for the M3 scenario.

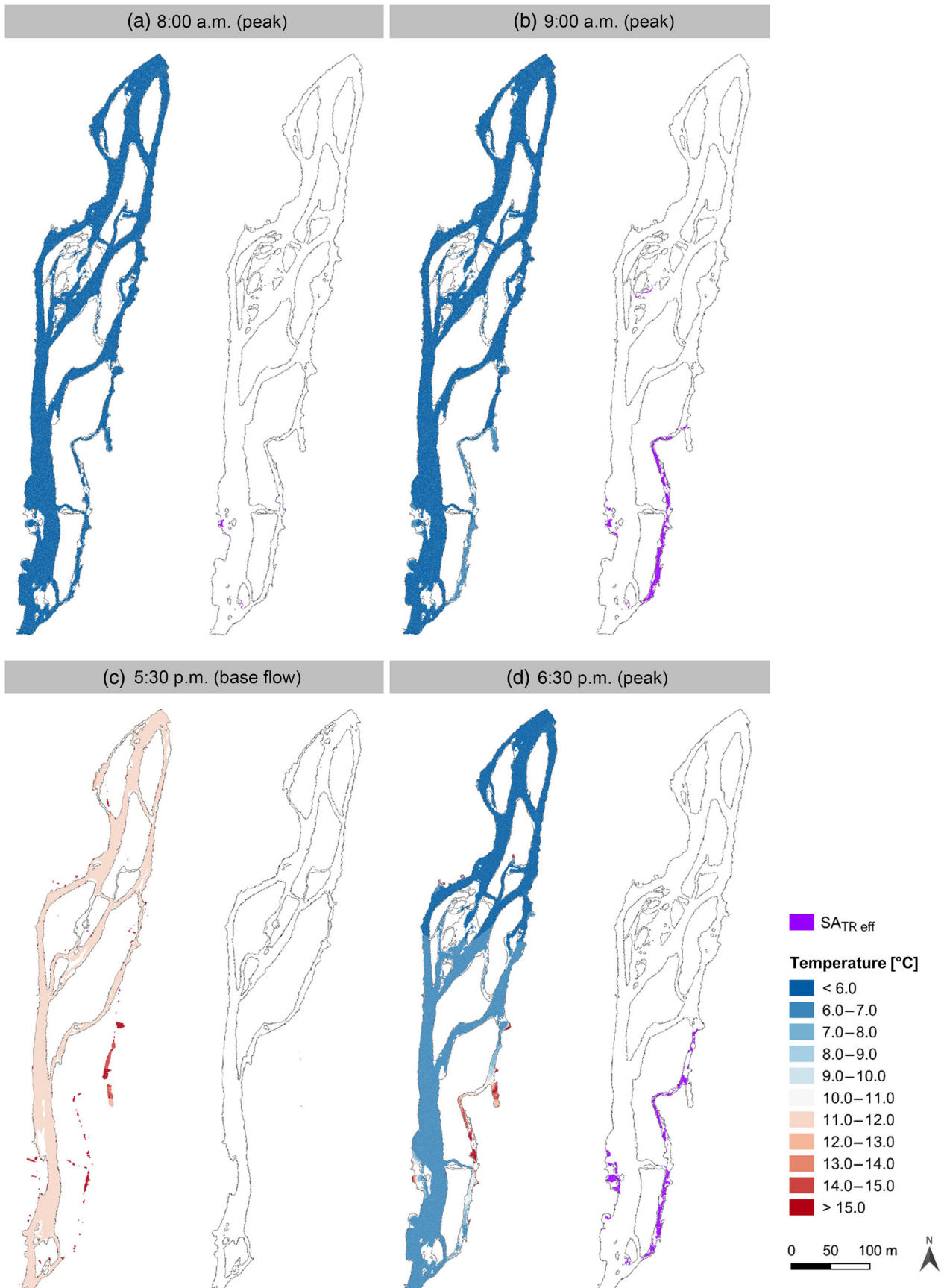


FIGURE 8 Example of spatial distributions of water temperature and effective suitable habitats for thermoregulation (SH_{TR,eff}) during different representative times of the day for the scenario M2_QR4_HP14_TP4 (see Table 1). (a and b) the first peak in the morning (amplitude 14 m³/s) is subdivided into two points in time; (c) base flow phase (4 m³/s) and (d) the second peak in the evening (amplitude 14 m³/s) [Color figure can be viewed at wileyonlinelibrary.com]

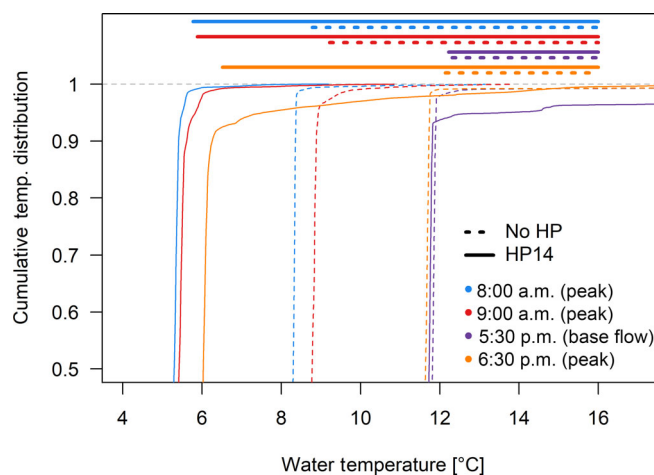


FIGURE 9 Upper part (0.5–1) of the cumulative water temperature distributions in the floodplain during different representative times of the day with (continuous lines; scenario M2_QR4_HP14_TP4 see Table 1) and without (dashed lines; scenario M2_QR4_HP0) hydropeaking. The horizontal segments represent the temperature ranges (i.e., the interval between $T_{w_median} + 0.5^{\circ}\text{C}$ and T_{w_pref}) used for defining the suitable habitats for thermoregulation (SH_{TR}) [Color figure can be viewed at wileyonlinelibrary.com]

3.2 | Habitat modelling under hydro- and thermo- and thermopeaking

In most simulation scenarios, the peak flow caused cold-thermo- and thermopeaking (Figure 6). Only the scenario TP8 led to a slight warming of the water temperature in the morning. During the peak phase, the CQV showed higher values compared to the scenario without hydropeaking. This value was higher the lower the temperature of turbine water and the higher the flow ratio was.

During the peak phases, SHA decreased in the base flow zone (Figure 7). The reduction was greater with a higher flow ratio. At the same time, new habitats formed temporarily in the dewatering zone. At the amplitude of $7\text{ m}^3/\text{s}$, the overall habitat availability remained lower than during base flow. Conversely, at the amplitude of $14\text{ m}^3/\text{s}$, new habitats compensated for the habitat losses in the base flow zone. When comparing base flow with peak flow conditions, the spatial distribution of hydraulically suitable habitats changed (Figure 7). At the amplitude of $7\text{ m}^3/\text{s}$, only 15% of the hydraulically suitable habitats remained stable. Most of these habitats were located along shallow gravel banks and in the side channels. At the amplitude of $14\text{ m}^3/\text{s}$, several new side channels were activated, and many new hydraulically suitable habitats were developed. However, only a small part (2%) of the habitats was stable.

Hydropeaking affected the thermal heterogeneity of the entire floodplain (Figures 6 and 8). After the marked cooling of the entire floodplain during the morning hydropeaking event, spatial heterogeneity emerged around noon. After the morning peak, however, disconnected habitats formed in the dewatering zone, and warmed up strongly during the day (Figure 8c). During the evening hydropeaking event, many of the isolated pools were flooded again and cooled down, an exception being those side channels that were not completely flooded. During and after the peak, they still had higher temperatures than the main channel. An increase in $SH_{TR,eff}$ was

observed in the side channels at a Q_{amp} of $14\text{ m}^3/\text{s}$ around 9:00 a.m. and 6:30 p.m., which corresponded to an increase in both thermal heterogeneity and the temperature range considered as SH_{TR} during the peak phase (Figure 9).

4 | DISCUSSION

4.1 | Spatiotemporal availability of suitable habitats

The simulation of synthetic hydrometeorological scenarios showed a pronounced water thermal heterogeneity in the Pomareda floodplain, which can be expected in a morphologically complex braided river floodplain (Arcott, Tockner, & Ward, 2001; Mosley, 1983; Tonolla, Acuña, Uehlinger, Frank, & Tockner, 2010; Uehlinger et al., 2003). Higher radiation intensities and larger air temperature amplitudes led to higher thermal heterogeneity. An increase in discharge reduced the thermal heterogeneity in the floodplain, as high discharges can cause the connection of individual water bodies, thereby homogenizing water temperatures (Ward, Tockner, Uehlinger, & Malard, 2001; Wawrzyniak et al., 2013; Webb, Hannah, Moore, Brown, & Nobilis, 2008). On the other hand, also very low discharges can lead to little hydro-morphological and thermal variability because all the flow occurs in a single main channel. This can lead to maximum thermal heterogeneity at intermediate discharges.

The SH_{TR} index was coupled in space and time with the thermal heterogeneity in the floodplain. The index showed a clear variation over the course of the day, with a maximum around noon and a decrease in the afternoon. This pattern originated because the side channels warmed up faster than the main channel in the first half of the day, whereas in the afternoon, the temperatures of the different river channels equalized. Juvenile brown trout, by exploiting the faster

warming areas in the side channels as habitats in early summer, could therefore benefit from warmer water temperatures for a longer period of time during the day, compared to their conspecifics in the main channel. This can lead to a potential growth advantage, provided that these habitats are detectable and reachable by fish. In the evening and at night, the thermal differences in the floodplain were small, meaning that there is hardly any suitable habitat for thermoregulation.

With increasing discharge, the overlap of thermally and hydraulically suitable habitats decreased. This can potentially lead to juvenile brown trout being exposed to a trade-off between thermally and hydraulically favourable habitats. The suitable habitats for thermoregulation were in fact found in the rather shallow and slowly flowing side channels. However, the use of these habitats may expose juvenile brown trout to an increased risk of predation by terrestrial predators (Crowder, Squires, & Rice, 1997).

4.2 | Impact of hydropeaking on the availability of suitable habitats

Hydraulically suitable habitats for juvenile fish were present during both base flow and peak flow phases in the Pomareda floodplain. As shown by Weber et al. (2015), morphologically intact braided floodplains seem to be able to buffer the negative effects of hydropeaking on habitat availability. This is due to side channels that can get activated during the up-ramping and peak phase, as well as shallow gravel banks which can get overflowed and, therefore, serve as temporary suitable habitat during hydropeaking. However, the interaction between hydropeaking and river morphology can have multiple and contrasting ecological effects (Vanzo, Zolezzi, & Siviglia, 2016). For example, the new habitats acting as refugia during peak flow can dry out during the down-ramping phase, increasing the risk of stranding (Auer, Zeiringer, Führer, Tonolla, & Schmutz, 2017; Halleraker et al., 2003; Vanzo, Tancon, Zolezzi, Alfredsen, & Siviglia, 2016). Our results showed that only a few hydraulically suitable habitats remained stable during hydropeaking. The higher the flow amplitude, the smaller the proportion of hydraulically stable habitats. Consequently, juvenile fish have to find new sites with every hydropeaking event, which can increase their energetic costs (Puffer et al., 2015). Several studies showed that hydropeaking affected the behaviour of fish, likely causing stress and forcing them to move to different habitats in response to flow changes (Boavida, Harby, Clarke, & Heggenes, 2017; Capra et al., 2017; Saltveit, Brabrand, Juárez, Stickler, & Dønnum, 2020; Scruton et al., 2003). Scruton et al. (2008) suggested that frequent changes in the habitat distribution may influence the survival of juvenile salmonids, especially in winter, as their body's energy reserves are lower. Reducing up- and down-ramping rates could give the fish more time to seek new suitable habitats (Halleraker et al., 2003). Due to the higher flow velocities during the peak phase, there is also a risk of fish being passively drifting downstream. Even if adult trout seem to be able to resist high flow velocities (Heggenes et al., 2007; Rocaspana, Aparicio, Palau-Ibars, Guillem, & Alcaraz, 2019), larvae and juvenile trout are more

susceptible to passive drift and stranding due to their still limited swimming ability (Auer et al., 2017; Thompson, Cocherell, Chun, Cech, & Klimley, 2011). Water temperature can further affect it, increasing the probability of passive drift and stranding at lower water temperatures (Halleraker et al., 2003; Heggenes & Traaen, 1988).

During the hydropeaking events, an increase in thermal heterogeneity was observed. The largest increase resulted in the scenario with the lowest temperature of the turbinated water (i.e., the largest temperature difference compared to the residual flow section). In contrast to the observed thermal heterogeneity without hydropeaking, this pattern is not due to natural heat exchange processes, but rather a consequence of the mixing between the warm water of the residual flow section and the cold turbinated water. Overall, the lower temperatures of the turbinated water led to a marked cooling within the floodplain. The extent of the cooling was mainly determined by the temperature of the turbinated water and less by the flow amplitude.

Although the defined hydropeaking scenarios led to strong changes in the spatial distribution of hydraulically suitable habitats in the floodplain, the variation of $SH_{TR,eff}$ over the course of the day was little affected, as the hydropeaking events occurred outside the phase with high thermal heterogeneity. However, after the down-ramping phase of the first hydropeaking event (in the morning), fragmented water areas originated in the dewatering zone, therefore increasing the risk of stranding as well as thermal stress (Elliott, 1981; Tuhtan, Noack, & Wieprecht, 2012). In more general terms, our results highlight how the thermal effects of hydro- and thermopeaking depend not only on the river morphology but also on the timing of such events.

4.3 | Value and potential improvements of thermal habitat modelling

Based on the assumption that a high thermal heterogeneity, as well as a large diversity of thermal habitats, can have positive effects on trout populations (McCullough et al., 2009), the indices we introduced (SH_{TR} and $SH_{TR,eff}$) successfully highlighted zones with temperatures that are closer to those for an optimal growth rate or growth efficiency, compared to average conditions. It is emphasized that habitat selection remains a trade-off between optimizing bioenergetics, food availability, shelter access, predator avoidance, and competition (Elliott & Allonby, 2013; Jonsson & Jonsson, 2011). According to McCullough et al. (2009), many questions related to the use of thermal refugia by salmonids remain open. These include the magnitude of the deviation from average conditions needed to gain a significant biological advantage, the circumstances under which thermal refugia are visited, as well as further characteristics (size, food availability, water chemistry, etc.) that thermal refugia need to have to be used by brown trout.

The presented interdisciplinary approach entails simplifications of the hydromorphological and ecological conditions in complex braided floodplains. The application of generalized HSC taken from the literature might be constrained in transferability, as suitability criteria can

differ seasonally as well as regionally and are often developed specifically for a given river reach (Person et al., 2014; Weber et al., 2015). However, especially for juveniles, it has been shown that data on habitat preferences can be transferred reliably between rivers (Nykanen & Huusko, 2004). The rate of temperature change and thermally stable habitats were not taken into account by SH_{TR} , although they are important parameters for the planning of hydropeaking mitigation measures (Carolli et al., 2012; Vanzo, Siviglia, Carolli, & Zolezzi, 2016). If the water temperature in suitable habitats changes too rapidly, the thermal wave could cause an avoidance response, forcing fish to seek new habitats to avoid the unfavourable temperatures (McCullough et al., 2009). Some thermally suitable habitats during the peak phase resulted in temperatures colder than areas considered non-suitable during base flow. To better highlight the criticalities of thermopeaking, however, SA_{TR} needs to be evaluated also in comparison with the temperature diurnal cycle without hydropeaking. In the next step, therefore, the absolute water temperatures, as well as their duration, will be included in the thermal habitat modelling.

5 | CONCLUSION AND OUTLOOK

Our results showed that the side channels in a morphologically semi-natural river floodplain are of great importance as fish habitats, as they not only show hydraulically suitable conditions under different discharge scenarios but also can be thermally beneficial for juvenile fish. To generalize these results, however, further synthetic scenarios with other hydrological and meteorological conditions need to be investigated. For example, a detailed analysis of the summer months, when water temperatures are warmer than those preferred by brown trout, or even exceed their upper tolerance threshold, would be of great interest in view of climate change (Muñoz-Mas, Lopez-Nicolas, Martínez-Capel, & Pulido-Velazquez, 2016; Santiago, Alonso, García de Jalón, Solana-Gutiérrez, & Muñoz-Mas, 2020). Moreover, analysing winter conditions would allow the development of brown trout eggs to be considered, which rely on stable temperature conditions and react sensitively to disturbances (Elliott, 1981).

To limit the influence of hydropeaking on thermal heterogeneity, the seasonal and diurnal operation regime could be modified to preferentially shift hydropeaking events outside of phases with high thermal heterogeneity. However, such a regime could lead to economic conflicts of interest (Casas-Mulet et al., 2016) because it limits the production flexibility of storage hydropower plants. Further investigations, as well as comparisons with natural scenarios, are therefore necessary to optimize as far as possible the cost–benefit ratio of such measures. Integrating 2D water temperature simulations in habitat modelling, as in the approach presented here, can help to better understand the effects of thermopeaking on fish habitat dynamics and, therefore, contribute to the ecological restoration of hydropower plants. Further, thanks to its reproducibility, our approach could be useful in the planning of restoration projects or to investigate the effects of climate change on discharge and water temperature.

ACKNOWLEDGEMENTS

This study was financially supported by the Swiss Federal Institute of Aquatic Science and Technology (Eawag). We would like to thank the operating company of the Soazza hydropower plant (Officine Idroelettriche di Mesolcina SA), which provided turbinated water flow data for our analysis and the Swiss Federal Office of Meteorology and Climatology MeteoSwiss for providing the meteorological data. We are also grateful to Patrick Paszti and Erik van Rooijen (ETH Zurich) for the setup and calibration of the hydrodynamic model, and to Victoria Scherelis for the English revision of the manuscript. Open access funding provided by Zurcher Hochschule fur Angewandte Wissenschaften.

DATA AVAILABILITY STATEMENT

The data that support the findings of this study are available from the corresponding author upon reasonable request.

ORCID

Manuel Antonetti  <https://orcid.org/0000-0002-4693-9908>

Diego Tonolla  <https://orcid.org/0000-0002-1172-0033>

Davide Vanzo  <https://orcid.org/0000-0002-2033-9197>

Martin Schmid  <https://orcid.org/0000-0001-8699-5691>

REFERENCES

- Angilletta, M. J., Jr., Ashley Steel, E., Bartz, K. K., Kingsolver, J. G., Scheuerell, M. D., Beckman, B. R., & Crozier, L. G. (2008). Big dams and salmon evolution: Changes in thermal regimes and their potential evolutionary consequences. *Evolutionary Applications*, 1(2), 286–299. <https://doi.org/10.1111/j.1752-4571.2008.00032.x>
- Armstrong, J. B., Schindler, D. E., Ruff, C. P., Brooks, G. T., Bentley, K. E., & Torgersen, C. E. (2013). Diel horizontal migration in streams: Juvenile fish exploit spatial heterogeneity in thermal and trophic resources. *Ecology*, 94(9), 2066–2075. <https://doi.org/10.1890/12-1200.1>
- Arcott, D. B., Tockner, K., & Ward, J. V. (2001). Thermal heterogeneity along a braided floodplain river (Tagliamento River, northeastern Italy). *Canadian Journal of Fisheries and Aquatic Sciences*, 58(12), 2359–2373. <https://doi.org/10.1139/cjfas-58-12-2359>
- Auer, S., Zeiringer, B., Führer, S., Tonolla, D., & Schmutz, S. (2017). Effects of river bank heterogeneity and time of day on drift and stranding of juvenile European grayling (*Thymallus thymallus* L.) caused by hydropeaking. *Science of the Total Environment*, 575, 1515–1521. <https://doi.org/10.1016/j.scitotenv.2016.10.029>
- Baldock, J. R., Armstrong, J. B., Schindler, D. E., & Carter, J. L. (2016). Juvenile coho salmon track a seasonally shifting thermal mosaic across a river floodplain. *Freshwater Biology*, 61(9), 1454–1465. <https://doi.org/10.1111/fwb.12784>
- Bejarano, M. D., Jansson, R., & Nilsson, C. (2018). The effects of hydropeaking on riverine plants: A review. *Biological Reviews*, 93(1), 658–673. <https://doi.org/10.1111/brv.12362>
- Berman, C. H., & Quinn, T. P. (1991). Behavioural thermoregulation and homing by spring chinook salmon, *Oncorhynchus tshawytscha* (Walbaum), in the Yakima River. *Journal of Fish Biology*, 39(3), 301–312. <https://doi.org/10.1111/j.1095-8649.1991.tb04364.x>
- Boavida, I., Harby, A., Clarke, K. D., & Heggenes, J. (2017). Move or stay: Habitat use and movements by Atlantic salmon parr (*Salmo salar*) during induced rapid flow variations. *Hydrobiologia*, 785(1), 261–275. <https://doi.org/10.1007/s10750-016-2931-3>
- Bonett, D. G. (2006). Confidence interval for a coefficient of quartile variation. *Computational Statistics & Data Analysis*, 50(11), 2953–2957. <https://doi.org/10.1016/j.csda.2005.05.007>

- Breau, C., Cunjak, R. A., & Bremset, G. (2007). Age-specific aggregation of wild juvenile Atlantic salmon *Salmo salar* at cool water sources during high temperature events. *Journal of Fish Biology*, 71(4), 1179–1191. <https://doi.org/10.1111/j.1095-8649.2007.01591.x>
- Brewitt, K. S., Danner, E. M., & Moore, J. W. (2017). Hot eats and cool creeks: Juvenile Pacific salmonids use mainstem prey while in thermal refuges. *Canadian Journal of Fisheries and Aquatic Sciences*, 74(10), 1588–1602. <https://doi.org/10.1139/cjfas-2016-0395>
- Bruder, A., Tonolla, D., Schweizer, S. P., Vollenweider, S., Langhans, S. D., & Wüest, A. (2016). A conceptual framework for hydropeaking mitigation. *Science of the Total Environment*, 568, 1204–1212. <https://doi.org/10.1016/j.scitotenv.2016.05.032>
- Bruno, M. C., Siviglia, A., Carolli, M., & Maiolini, B. (2013). Multiple drift responses of benthic invertebrates to interacting hydropeaking and thermopeaking waves. *Ecohydrology*, 6(4), 511–522. <https://doi.org/10.1002/eco.1275>
- Caissie, D. (2006). The thermal regime of rivers: A review. *Freshwater Biology*, 51(8), 1389–1406. <https://doi.org/10.1111/j.1365-2427.2006.01597.x>
- Capra, H., Plichard, L., Bergé, J., Pella, H., Ovidio, M., McNeil, E., & Lamouroux, N. (2017). Fish habitat selection in a large hydropeaking river: Strong individual and temporal variations revealed by telemetry. *Science of the Total Environment*, 578, 109–120. <https://doi.org/10.1016/j.scitotenv.2016.10.155>
- Carolli, M., Bruno, M. C., Siviglia, A., & Maiolini, B. (2012). Responses of benthic invertebrates to abrupt changes of temperature in flume simulations. *River Research and Applications*, 28(6), 678–691. <https://doi.org/10.1002/rra.1520>
- Casas-Mulet, R., Saltveit, S. J., & Alfredsen, K. T. (2016). Hydrological and thermal effects of hydropeaking on early life stages of salmonids: A modelling approach for implementing mitigation strategies. *Science of the Total Environment*, 573, 1660–1672. <https://doi.org/10.1016/j.scitotenv.2016.09.208>
- Clarkson, R. W., & Childs, M. R. (2000). Temperature effects of hypolimnial-release dams on early life stages of Colorado river basin big-river fishes. *Copeia*, 2, 402–412.
- Crowder, L., Squires, D., & Rice, J. (1997). Nonadditive effects of terrestrial and aquatic predators on juvenile estuarine fish. *Ecology*, 78, 1796–1804. <https://doi.org/10.2307/2266102>
- Eberstaller, J., Frangez, C., Schneider, M., Kopecki, I., Baumann, P., & Wächter, K. (2012). *Alpenrhein D6. Quantitative Analyse von Schwall-/Sunk-Ganglinien für unterschiedliche Anforderungsprofile. Arbeitspaket 5–Habitatmodellierung zur quantitativen Bewertung der Größe des Schwalleneinflusses am Alpenrhein* [Report commissioned by IRKA]. Vienna, Zurich, Stuttgart. Retrieved from https://www.alpenrhein.net/Portals/0/Content/20120312_D6_Alpenrhein_AP5_END-1.pdf
- Elliott, J. M. (1981). Some aspects of thermal stress on freshwater Teleosts. In A. D. Pickering (Ed.), *Stress in fish* (pp. 209–249). London, England: Academic Press.
- Elliott, J. M., & Allonby, J. D. (2013). An experimental study of ontogenetic and seasonal changes in the temperature preferences of unfed and fed brown trout, *Salmo trutta*. *Freshwater Biology*, 58(9), 1840–1848. <https://doi.org/10.1111/fwb.12173>
- Federal Office of Meteorology and Climatology MeteoSwiss. (2020). *Meteorological data*. Retrieved from <http://www.meteoswiss.admin.ch/>
- Feng, M., Zolezzi, G., & Pusch, M. (2018). Effects of thermopeaking on the thermal response of alpine river systems to heatwaves. *Science of the Total Environment*, 612, 1266–1275. <https://doi.org/10.1016/j.scitotenv.2017.09.042>
- García, A., Jorde, K., Habit, E., Caamaño, D., & Parra, O. (2011). Downstream environmental effects of dam operations: Changes in habitat quality for native fish species. *River Research and Applications*, 27(3), 312–327. <https://doi.org/10.1002/rra.1358>
- Grand, T. C., Railsback, S. F., Hayse, J. W., & LaGory, K. E. (2006). A physical habitat model for predicting the effects of flow fluctuations in nursery habitats of the endangered Colorado pikeminnow (*Ptychocheilus lucius*). *River Research and Applications*, 22(10), 1125–1142. <https://doi.org/10.1002/rra.967>
- Greimel, F., Zeiringer, B., Höller, N., Grün, B., Godina, R., & Schmutz, S. (2016). A method to detect and characterize sub-daily flow fluctuations. *Hydrological Processes*, 30(13), 2063–2078. <https://doi.org/10.1002/hyp.10773>
- Halleraker, J. H., Saltveit, S. J., Harby, A., Arnekleiv, J. V., Fjeldstad, H.-P., & Kohler, B. (2003). Factors influencing stranding of wild juvenile brown trout (*Salmo trutta*) during rapid and frequent flow decreases in an artificial stream. *River Research and Applications*, 19(5–6), 589–603. <https://doi.org/10.1002/rra.752>
- Hauer, C., Unfer, G., Holzapfel, P., Haimann, M., & Habersack, H. (2014). Impact of channel bar form and grain size variability on estimated stranding risk of juvenile brown trout during hydropeaking. *Earth Surface Processes and Landforms*, 39(12), 1622–1641. <https://doi.org/10.1002/esp.3552>
- Heggernes, J., Alfredsen, K., Bustos, A. A., Huusko, A., & Stickler, M. (2018). Be cool: A review of hydro-physical changes and fish responses in winter in hydropower-regulated northern streams. *Environmental Biology of Fishes*, 101(1), 1–21. <https://doi.org/10.1007/s10641-017-0677-z>
- Heggernes, J., Omholt, P. K., Kristiansen, J. R., Sageie, J., Økland, F., Dokk, J. G., & Beere, M. C. (2007). Movements by wild brown trout in a boreal river: Response to habitat and flow contrasts. *Fisheries Management and Ecology*, 14(5), 333–342. <https://doi.org/10.1111/j.1365-2400.2007.00559.x>
- Heggernes, J., & Traaen, T. (1988). Downstream migration and critical water velocities in stream channels for fry of four salmonid species. *Journal of Fish Biology*, 32(5), 717–727. <https://doi.org/10.1111/j.1095-8649.1988.tb05412.x>
- Huet, M. (1949). Aperçu des relations entre la pente et les populations piscicoles des eaux courantes. *Schweizerische Zeitschrift für Hydrologie*, 11(3), 332–351. <https://doi.org/10.1007/BF02503356>
- International Energy Agency. (2019). *Electricity production*. Retrieved from <https://www.iea.org/reports/electricity-information-overview/electricity-production>
- Jonsson, B., & Jonsson, N. (2009). A review of the likely effects of climate change on anadromous Atlantic salmon *Salmo salar* and brown trout *Salmo trutta*, with particular reference to water temperature and flow. *Journal of Fish Biology*, 75(10), 2381–2447. <https://doi.org/10.1111/j.1095-8649.2009.02380.x>
- Jonsson, B., & Jonsson, N. (2011). *Ecology of Atlantic Salmon and Brown trout: Habitat as a template for life histories*. Dordrecht, The Netherlands: Springer. <https://doi.org/10.1007/978-94-007-1189-1>
- Macura, V., Štefunková, Z., Majorošová, M., Halaj, P., & Škrinář, A. (2018). Influence of discharge on fish habitat suitability curves in mountain watercourses in IFIM methodology. *Journal of Hydrology and Hydromechanics*, 66, 12–22. <https://doi.org/10.1515/johh-2017-0044>
- Malard, F., Mangin, A., Uehlinger, U., & Ward, J. V. (2001). Thermal heterogeneity in the hyporheic zone of a glacial floodplain. *Canadian Journal of Fisheries and Aquatic Sciences*, 58(7), 1319–1335. <https://doi.org/10.1139/f01-079>
- McCullough, D. A., Bartholow, J. M., Jager, H. I., Beschta, R. L., Cheslak, E. F., Deas, M. L., ... Wurtsbaugh, W. A. (2009). Research in thermal biology: Burning questions for coldwater stream fishes. *Reviews in Fisheries Science*, 17(1), 90–115. <https://doi.org/10.1080/10641260802590152>
- Meier, W., Bonjour, C., Wüest, A., & Reichert, P. (2003). Modeling the effect of water diversion on the temperature of mountain streams. *Journal of Environmental Engineering, ASCE*, 129(8), 755–764. [https://doi.org/10.1061/\(ASCE\)0733-9372\(2003\)129:8\(755\)](https://doi.org/10.1061/(ASCE)0733-9372(2003)129:8(755))
- Moreira, M., Hayes, D. S., Boavida, I., Schletterer, M., Schmutz, S., & Pinheiro, A. (2019). Ecologically-based criteria for hydropeaking mitigation: A review. *Science of the Total Environment*, 657, 1508–1522. <https://doi.org/10.1016/j.scitotenv.2018.12.107>

- Mosley, M. P. (1983). Variability of water temperatures in the braided Ashley and Rakaia rivers. *New Zealand Journal of Marine and Freshwater Research*, 17(3), 331–342. <https://doi.org/10.1080/00288330.1983.9516007>
- Muñoz-Mas, R., Lopez-Nicolas, A., Martínez-Capel, F., & Pulido-Velazquez, M. (2016). Shifts in the suitable habitat available for brown trout (*Salmo trutta* L.) under short-term climate change scenarios. *Science of the Total Environment*, 544, 686–700. <https://doi.org/10.1016/j.scitotenv.2015.11.147>
- Muñoz-Mas, R., Martínez-Capel, F., Schneider, M., & Mouton, A. M. (2012). Assessment of brown trout habitat suitability in the Jucar River Basin (SPAIN): Comparison of data-driven approaches with fuzzy-logic models and univariate suitability curves. *Science of the Total Environment*, 440, 123–131. <https://doi.org/10.1016/j.scitotenv.2012.07.074>
- Nykanen, M., & Huusko, A. (2004). Transferability of habitat preference criteria for larval European grayling (*Thymallus thymallus*). *Canadian Journal of Fisheries and Aquatic Sciences*, 61(2), 185–192. <https://doi.org/10.1139/F03-156>
- Olden, J. D., & Naiman, R. J. (2010). Incorporating thermal regimes into environmental flows assessments: Modifying dam operations to restore freshwater ecosystem integrity. *Freshwater Biology*, 55(1), 86–107. <https://doi.org/10.1111/j.1365-2427.2009.02179.x>
- Olsen, D. A., & Young, R. G. (2009). Significance of river-aquifer interactions for reach-scale thermal patterns and trout growth potential in the Motueka River, New Zealand. *Hydrogeology Journal*, 17(1), 175–183. <https://doi.org/10.1007/s10040-008-0364-4>
- Ouellet, V., Secretan, Y., St-Hilaire, A., & Morin, J. (2014). Daily averaged 2d water temperature model for the St. Lawrence River. *River Research and Applications*, 30(6), 733–744. <https://doi.org/10.1002/rra.2664>
- Ouellet, V., St-Hilaire, A., Dugdale, S. J., Hannah, D. M., Krause, S., & Proulx-Ouellet, S. (2020). River temperature research and practice: Recent challenges and emerging opportunities for managing thermal habitat conditions in stream ecosystems. *Science of the Total Environment*, 736, 139679. <https://doi.org/10.1016/j.scitotenv.2020.139679>
- Paszti, P. (2019). *Study of fish mesohabitat dynamics in the Moesa river*. (Master thesis). ETHZ/Laboratory of Hydraulics, Hydrology and Glaciology VAW, Zürich.
- Person, E., Bieri, M., Peter, A., & Schleiss, A. J. (2014). Mitigation measures for fish habitat improvement in Alpine rivers affected by hydropower operations. *Ecohydrology*, 7(2), 580–599. <https://doi.org/10.1002/eco.1380>
- Petty, J. T., Hansbarger, J. L., Huntsman, B. M., & Mazik, P. M. (2012). Brook trout movement in response to temperature, flow, and thermal refugia within a complex Appalachian riverscape. *Transactions of the American Fisheries Society*, 141(4), 1060–1073. <https://doi.org/10.1080/00028487.2012.681102>
- Pisaturo, G. R., Righetti, M., Dumbser, M., Noack, M., Schneider, M., & Cavedon, V. (2017). The role of 3D-hydraulics in habitat modelling of hydropneaking events. *Science of the Total Environment*, 575, 219–230. <https://doi.org/10.1016/j.scitotenv.2016.10.046>
- Pix4D. (2020). Pix4Dmapper: Professional drone mapping and photogrammetry software. Retrieved from <https://www.pix4d.com/product/pix4dmapper-photogrammetry-software>
- Poff, N. L., Allan, J. D., Bain, M. B., Karr, J. R., Prestegard, K. L., Richter, B. D., ... Stromberg, J. C. (1997). The natural flow regime. *BioScience*, 47(11), 769–784. <https://doi.org/10.2307/1313099>
- Puffer, M., Berg, O. K., Huusko, A., Vehanen, T., Forseth, T., & Einum, S. (2015). Seasonal effects of hydropneaking on growth, energetics and movement of juvenile Atlantic Salmon (*Salmo Salar*). *River Research and Applications*, 31(9), 1101–1108. <https://doi.org/10.1002/rra.2801>
- Quinn, J. W., & Kwak, T. J. (2003). Fish assemblage changes in an Ozark River after impoundment: A long-term perspective. *Transactions of the American Fisheries Society*, 132(1), 110–119. [https://doi.org/10.1577/1548-8659\(2003\)132<0110:FCIAO>2.0.CO;2](https://doi.org/10.1577/1548-8659(2003)132<0110:FCIAO>2.0.CO;2)
- Rocaspana, R., Aparicio, E., Palau-Ibars, A., Guillem, R., & Alcaraz, C. (2019). Hydropneaking effects on movement patterns of brown trout (*Salmo trutta* L.). *River Research and Applications*, 35(6), 646–655. <https://doi.org/10.1002/rra.3432>
- Saltveit, S. J. (1990). Effect of decreased temperature on growth and smoltification of juvenile Atlantic salmon (*Salmo salar*) and brown trout (*Salmo trutta*) in a norwegian regulated river. *Regulated Rivers: Research & Management*, 5(4), 295–303. <https://doi.org/10.1002/rrr.3450050402>
- Saltveit, S. J., Brabrand, Å., Juárez, A., Stickler, M., & Dønnum, B. O. (2020). The impact of hydropneaking on juvenile brown trout (*Salmo trutta*) in a Norwegian regulated river. *Sustainability*, 12(20), 8670. <https://doi.org/10.3390/su12208670>
- Saltveit, S. J., Halleraker, J. H., Arnekleiv, J. V., & Harby, A. (2001). Field experiments on stranding in juvenile Atlantic salmon (*Salmo salar*) and brown trout (*Salmo trutta*) during rapid flow decreases caused by hydropneaking. *Regulated Rivers: Research & Management*, 17(4–5), 609–622. <https://doi.org/10.1002/rrr.652>
- Santiago, J. M., Alonso, C., García de Jalón, D., Solana-Gutiérrez, J., & Muñoz-Mas, R. (2020). Effects of climate change on the life stages of stream-dwelling brown trout (*Salmo trutta* Linnaeus, 1758) at the rear edge of their native distribution range. *Ecohydrology*, 13(7), e2241. <https://doi.org/10.1002/eco.2241>
- Schmutz, S., Bakken, T. H., Friedrich, T., Greimel, F., Harby, A., Jungwirth, M., ... Zeiringer, B. (2015). Response of fish communities to hydrological and morphological alterations in hydropneaking Rivers of Austria. *River Research and Applications*, 31(8), 919–930. <https://doi.org/10.1002/rra.2795>
- Scruton, D. A., Ollerhead, L. M. N., Clarke, K. D., Pennell, C., Alfredsen, K., Harby, A., & Kelley, D. (2003). The behavioural response of juvenile Atlantic salmon (*Salmo salar*) and brook trout (*Salvelinus fontinalis*) to experimental hydropneaking on a Newfoundland (Canada) river. *River Research and Applications*, 19(5–6), 577–587. <https://doi.org/10.1002/rra.733>
- Scruton, D. A., Pennell, C., Ollerhead, L. M. N., Alfredsen, K., Stickler, M., Harby, A., ... LeDrew, L. J. (2008). A synopsis of 'hydropneaking' studies on the response of juvenile Atlantic salmon to experimental flow alteration. *Hydrobiologia*, 609(1), 263–275. <https://doi.org/10.1007/s10750-008-9409-x>
- SEBA Hydrometrie GmbH & Co. (2021). SEBA internetmodul. Retrieved from <https://www.seba-hydrocenter.de>
- Swiss Federal Office of Energy. (2020). *Energy strategy 2050—Monitoring report 2020*. Ittigen, Switzerland: Author.
- Thompson, L. C., Cocherell, S. A., Chun, S. N., Cech, J. J., & Klimley, A. P. (2011). Longitudinal movement of fish in response to a single-day flow pulse. *Environmental Biology of Fishes*, 90(3), 253–261. <https://doi.org/10.1007/s10641-010-9738-2>
- Toffolon, M., Siviglia, A., & Zolezzi, G. (2010). Thermal wave dynamics in rivers affected by hydropneaking. *Water Resources Research*, 46(8), 1–18. <https://doi.org/10.1029/2009WR008234>
- Tonolla, D., Acuña, V., Uehlinger, U., Frank, T., & Tockner, K. (2010). Thermal heterogeneity in river floodplains. *Ecosystems*, 13(5), 727–740. <https://doi.org/10.1007/s10021-010-9350-5>
- Tuhtan, J. A., Noack, M., & Wieprecht, S. (2012). Estimating stranding risk due to hydropneaking for juvenile European grayling considering river morphology. *KSCE Journal of Civil Engineering*, 16(2), 197–206. <https://doi.org/10.1007/s12205-012-0002-5>
- Uehlinger, U., Malard, F., & Ward, J. V. (2003). Thermal patterns in the surface waters of a glacial river corridor (Val Roseg, Switzerland). *Freshwater Biology*, 48(2), 284–300. <https://doi.org/10.1046/j.1365-2427.2003.01000.x>
- van Rooijen, E. (2022). *Development and application of a new automatic fluvial mesohabitat approach* (Doctoral Thesis). ETH Zurich. <https://doi.org/10.3929/ethz-b-000541091>

- Vanzo, D., Peter, S., Vonwiller, L., Bürgler, M., Weberndorfer, M., Siviglia, A., ... Vetsch, D. F. (2021). BASEMENT v3: A modular freeware for river process modelling over multiple computational backends. *Environmental Modelling & Software*, 143, 105102. <https://doi.org/10.1016/j.envsoft.2021.105102>
- Vanzo, D., Siviglia, A., Carolli, M., & Zolezzi, G. (2016). Characterization of sub-daily thermal regime in alpine rivers: Quantification of alterations induced by hydropowering. *Hydrological Processes*, 30(7), 1052–1070. <https://doi.org/10.1002/hyp.10682>
- Vanzo, D., Siviglia, A., & Toro, E. F. (2016). Pollutant transport by shallow water equations on unstructured meshes: Hyperbolization of the model and numerical solution via a novel flux splitting scheme. *Journal of Computational Physics*, 321, 1–20. <https://doi.org/10.1016/j.jcp.2016.05.023>
- Vanzo, D., Tancon, M., Zolezzi, G., Alfredsen, K., & Siviglia, A. (2016). *Modeling approach for the quantification of fish stranding risk: The case of Lundesokna river (Norway)*. Paper presented at the 11th ISE, Melbourne, Australia.
- Vanzo, D., Zolezzi, G., & Siviglia, A. (2016). Eco-hydraulic modelling of the interactions between hydropowering and river morphology. *Ecohydrology*, 9(3), 421–437. <https://doi.org/10.1002/eco.1647>
- Wakeley, J. S. (1988). A method to create simplified versions of existing habitat suitability index (HSI) models. *Environmental Management*, 12(1), 79–83. <https://doi.org/10.1007/BF01867379>
- Ward, J. V., Tockner, K., Uehlinger, U., & Malard, F. (2001). Understanding natural patterns and processes in river corridors as the basis for effective river restoration. *Regulated Rivers: Research & Management*, 17(4–5), 311–323. <https://doi.org/10.1002/rrr.646>
- Wawrzyniak, V., Piégay, H., Allemand, P., Vaudor, L., Goma, R., & Grandjean, P. (2016). Effects of geomorphology and groundwater level on the spatio-temporal variability of riverine cold water patches assessed using thermal infrared (TIR) remote sensing. *Remote Sensing of Environment*, 175, 337–348. <https://doi.org/10.1016/j.rse.2015.12.050>
- Wawrzyniak, V., Piégay, H., Allemand, P., Vaudor, L., & Grandjean, P. (2013). Prediction of water temperature heterogeneity of braided rivers using very high resolution thermal infrared (TIR) images. *International Journal of Remote Sensing*, 34(13), 4812–4831. <https://doi.org/10.1080/01431161.2013.782113>
- Webb, B. W., Hannah, D. M., Moore, R. D., Brown, L. E., & Nobilis, F. (2008). Recent advances in stream and river temperature research. *Hydrological Processes*, 22(7), 902–918. <https://doi.org/10.1002/hyp.6994>
- Weber, C., Schneider, M., Junker, J., Kopecki, I., & Alexander, T. (2015). *Modelling fish habitat dynamics in hydropowering rivers considering different morphology and habitat requirements. Current state, needs for improvement, and guidelines for application* (No. SI/500959-01) (p. 40). Bern, Switzerland: Bundesamt für Energie BFE.
- Wilbur, N. M., O'Sullivan, A. M., MacQuarrie, K. T. B., Linnansaari, T., & Curry, R. A. (2020). Characterizing physical habitat preferences and thermal refuge occupancy of brook trout (*Salvelinus fontinalis*) and Atlantic salmon (*Salmo salar*) at high river temperatures. *River Research and Applications*, 1–15, 769–783. <https://doi.org/10.1002/rra.3570>
- Wohl, E., Bledsoe, B. P., Jacobson, R. B., Poff, N. L., Rathburn, S. L., Walters, D. M., & Wilcox, A. C. (2015). The natural sediment regime in rivers: Broadening the foundation for ecosystem management. *Bioscience*, 65(4), 358–371. <https://doi.org/10.1093/biosci/biv002>
- Yao, W.-W., Chen, Y., Zhong, Y., Zhang, W., & Fan, H. (2017). Habitat models for assessing river ecosystems and their application to the development of river restoration strategies. *Journal of Freshwater Ecology*, 32(1), 601–617. <https://doi.org/10.1080/02705060.2017.1371088>
- Young, P. S., Cech, J. J., & Thompson, L. C. (2011). Hydropower-related pulsed-flow impacts on stream fishes: A brief review, conceptual model, knowledge gaps, and research needs. *Reviews in Fish Biology and Fisheries*, 21(4), 713–731. <https://doi.org/10.1007/s11160-011-9211-0>
- Zhong, Y., & Power, G. (1996). Environmental impacts of hydroelectric projects on fish resources in China. *Regulated Rivers: Research & Management*, 12(1), 81–98. [https://doi.org/10.1002/\(SICI\)1099-1646\(199601\)12:1<81::AID-RRR378>3.0.CO;2-9](https://doi.org/10.1002/(SICI)1099-1646(199601)12:1<81::AID-RRR378>3.0.CO;2-9)
- Zolezzi, G., Siviglia, A., Toffolon, M., & Maiolini, B. (2011). Thermopeaking in Alpine streams: Event characterization and time scales. *Ecohydrology*, 4(4), 564–576. <https://doi.org/10.1002/eco.132>

SUPPORTING INFORMATION

Additional supporting information can be found online in the Supporting Information section at the end of this article.

How to cite this article: Antonetti, M., Hoppler, L., Tonolla, D., Vanzo, D., Schmid, M., & Doering, M. (2022). Integrating two-dimensional water temperature simulations into a fish habitat model to improve hydro- and thermopeaking impact assessment. *River Research and Applications*, 1–21. <https://doi.org/10.1002/rra.4043>

APPENDIX

TABLE A1 List of abbreviations used in this study

Abbreviation	Long name/description
2D	Two-dimensional
BC	Boundary conditions
CQV	Coefficient of quartile variation (%)
DEM	Digital elevation model
GR	Global radiation (W/m^2)
h	Water depth (m)
HP0, HP7, HP14	Hydropeaking scenarios
HSC	Habitat suitability curves
HSI	Habitat suitability index (–)
M1, M2, M3	Meteorological scenarios
Q	Discharge (m^3/s)
Q_{amp}	Amplitude of the hydropeaking event (m^3/s)
Q_{base}	Base flow (m^3/s)
Q_{peak}	Peak flow (m^3/s)
Q_{turb}	Turbined water flow (m^3/s); $0 < Q_{\text{turb}} < Q_{\text{amp}}$
QR2, QR4, QR6	Scenarios defined based on hydrological conditions in the residual flow section
SHA	Suitable habitat area (m^2)
SHR	Suitable habitat ratio (–)
SHR_{TR}	Suitable habitat ratio for thermoregulation (–)
SH_{TR}	Suitable habitats for thermoregulation (m^2)
$\text{SH}_{\text{TR,eff}}$	Effective suitable habitats for thermoregulation (m^2)
T_{a}	Air temperature ($^{\circ}\text{C}$)
$T_{\text{a,amp}}$	Amplitude, that is, max. deviation from $T_{\text{a,mean}}$ ($^{\circ}\text{C}$)
$T_{\text{a,mean}}$	Mean daily air temperature ($^{\circ}\text{C}$)
TIR	Thermal infrared
TP4, TP6, TP8	Thermo peaking scenarios
$T_{\text{w,pref}}$	Preferential temperature ($^{\circ}\text{C}$)
T_{w}	Water temperature ($^{\circ}\text{C}$)
$T_{\text{w,rfs}}$	Water temperature or the residual flow section ($^{\circ}\text{C}$)
$T_{\text{w,amp}}$	Amplitude, that is, max. deviation from $T_{\text{w,mean}}$ ($^{\circ}\text{C}$)
$T_{\text{w,mean}}$	Mean daily water temperature ($^{\circ}\text{C}$)
$T_{\text{w,median}}$	Median of water temperature ($^{\circ}\text{C}$)
$T_{\text{w,TP}}$	Temperature of the water turbined from the hydropower plant ($^{\circ}\text{C}$)
v	Flow velocity (m/s)
WA	Wetted area (m^2)

TABLE A2 Formal expressions of the indices used for the fish habitat modelling

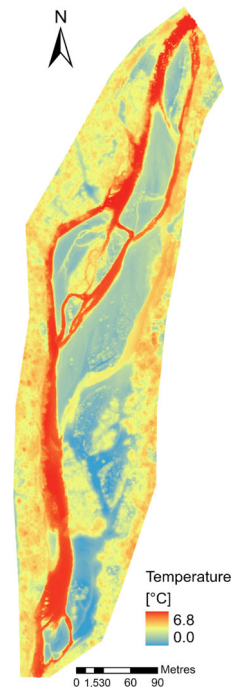
Index	Extended name	Equation
HSI	Habitat suitability index (-)	$HSI = \sqrt{SI_h \cdot SI_v}$
SHA	Suitable habitat area (m ²)	$SHA = \sum_{i=1}^n A_i \mid HSI_i > 0.5$
WA	Wetted area (m ²)	$WA = \sum_{i=1}^n A_i \mid h_i > 0.05 \text{ m}$
SHR	Suitable habitat ratio (-)	$SHR = SHA/WA$
SH _{TR}	Suitable habitats for thermoregulation (m ²)	$SH_{TR} = \sum_{i=1}^n A_i \mid \Delta T_{wi} > 0.5^\circ \text{ C and } T_{wi} \leq T_{w_pref}$
SH _{TR_eff}	Effective suitable habitats for thermoregulation (m ²)	$SHA \cap SH_{TR}$

Abbreviations: ΔT_{w_i} , thermal anomaly, that is, the difference between the temperature of a computational cell and the median (T_{w_median}) of all computational cells within a 2 m buffer around the centreline of the main channel; A_i , area of computation cell; SI_h , suitability index of water depth; SI_v , suitability index of velocity; T_{w_i} , water temperature. T_{w_pref} , preferential water temperature; WA, wetted area.

TABLE A3 Formal equations used for the design of the simulation scenarios

Description	Equation
Gaussian function used for the synthetic time series of global radiation	$GR(t) = GR_{max} \cdot \exp\left(-a\left(\frac{t-b}{c}\right)^2\right)$
Sine function for the synthetic time series of air and water temperature	$T_i(t) = T_{i_mean} + T_{i_amp} \cdot \sin\left(\frac{2\pi}{T_C}t + \Phi_0\right)$
Mixing ratio of discharge and temperature	$T_{w_input}(t) = \frac{Q_{base} \cdot T_{w_rfs}(t) + Q_{turb}(t) \cdot T_{w_TP}}{Q_{base} + Q_{turb}(t)}$

Abbreviations: a , curvature parameter of the curve, set equal to 50; b , position of the centre of the peak, set equal to 11.5 hr; c , period duration, set equal to 24 hr; GR, global radiation (W/m²); GR_{max} , daily maximum of global radiation (W/m²); Q_{turb} , turbined water flow (m³/s), with $0 < Q_{turb} < Q_{amp}$; T_i , air/water temperature (°C); T_{i_mean} , mean daily water temperature (°C); T_{i_amp} , amplitude, that is, max. deviation from T_{i_mean} (°C); Φ_0 , phase angle set equal to 21.5 hr (22.5 hr) for air (water) temperature; T_{w_input} , input water temperature (°C); T_{w_rfs} , water temperature of the residual flow section (°C); T_{w_TP} , temperature of the water turbined from the hydropower plant (°C).

**FIGURE A1** Thermal infrared (TIR) mosaic derived with a UAV survey on February 7, 2019 at ca. 8:00 a.m. during base flow condition. Flow direction from north to south [Color figure can be viewed at wileyonlinelibrary.com]

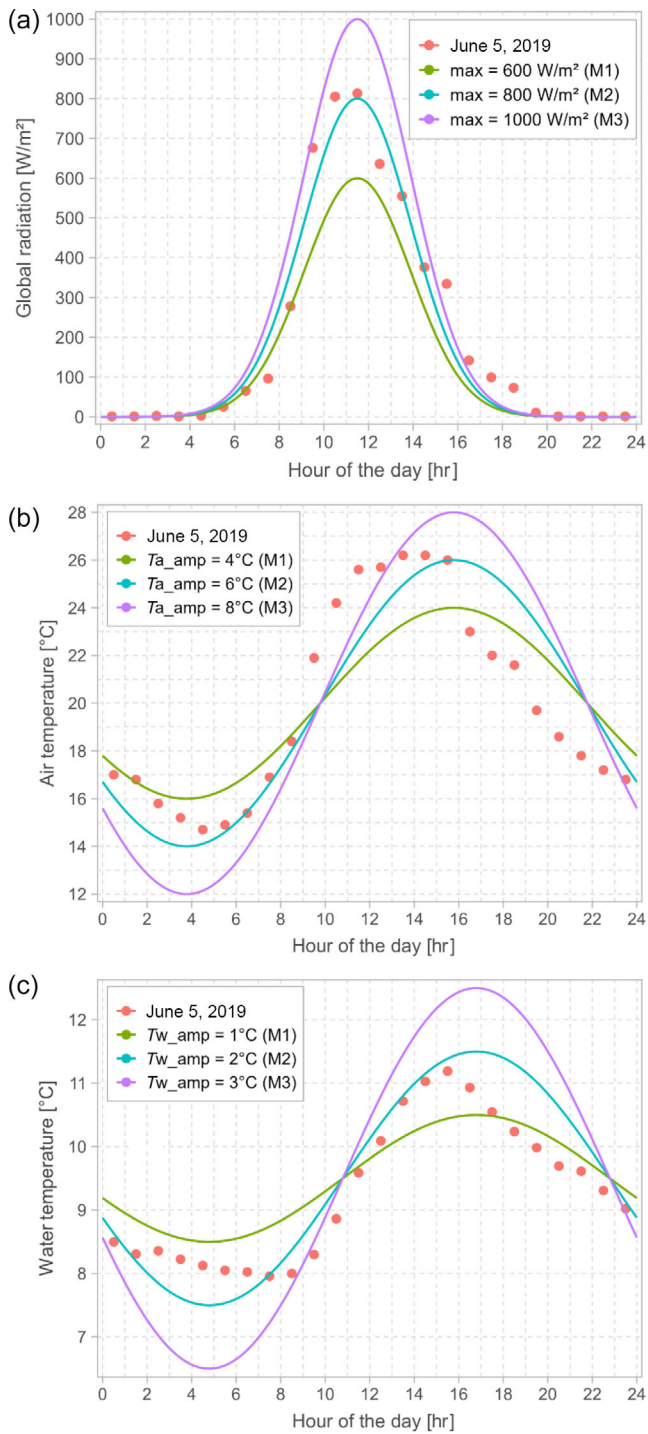


FIGURE A2 Overview of the meteorological scenarios defined for this study. Starting from the scenario (M2) that best corresponded to a representative day (5 June 2019), two further scenarios were defined for global radiation (a), air temperature (b), and water temperature (c), with smaller (M1) and larger (M3) maximum values and amplitudes, respectively. The equations used to derive the meteorological scenarios are listed in Table A3 [Color figure can be viewed at wileyonlinelibrary.com]

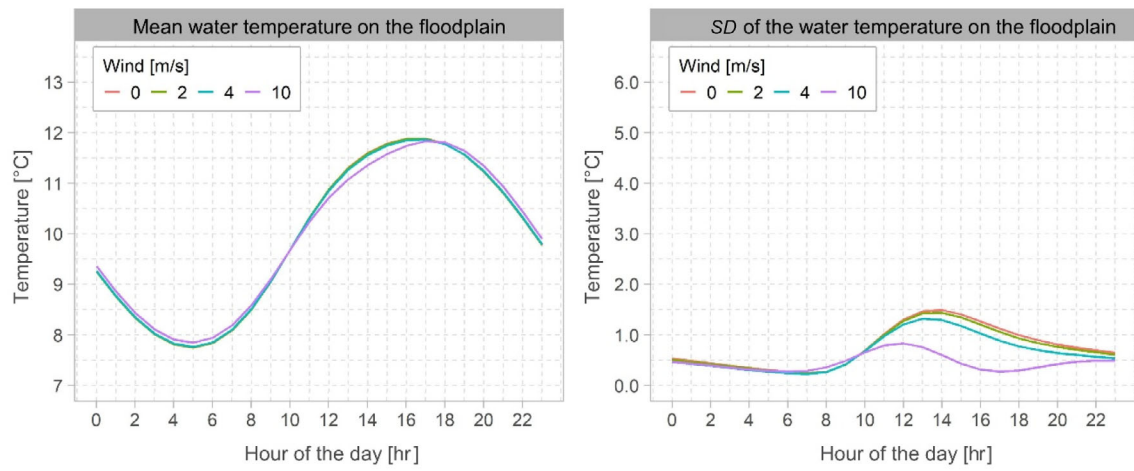


FIGURE A3 Mean (left) and *SD* (right) of the simulated water temperature over the entire floodplain over the course of the day as a function of the wind speed [Color figure can be viewed at wileyonlinelibrary.com]